J. Fluid Mech. (2013), *vol.* 734, *pp.* 83–113.
doi:10.1017/jfm.2013.458

Global analysis of Navier–Stokes and Boussinesq stochastic flows using dynamical orthogonality

T. P. Sapsis[1,2,†], M. P. Ueckermann[1] and P. F. J. Lermusiaux[1]

[1]Department of Mechanical Engineering, Massachusetts Institute of Technology, 77 Massachusetts Avenue, Cambridge, MA 02139, USA

[2]Courant Institute of Mathematical Sciences, New York University, 251 Mercer Street, New York, NY 10012, USA

(Received 22 September 2012; revised 23 July 2013; accepted 31 August 2013)

We provide a new framework for the study of fluid flows presenting complex uncertain behaviour. Our approach is based on the stochastic reduction and analysis of the governing equations using the dynamically orthogonal field equations. By numerically solving these equations, we evolve in a fully coupled way the mean flow and the statistical and spatial characteristics of the stochastic fluctuations. This set of equations is formulated for the general case of stochastic boundary conditions and allows for the application of projection methods that considerably reduce the computational cost. We analyse the transformation of energy from stochastic modes to mean dynamics, and vice versa, by deriving exact expressions that quantify the interaction among different components of the flow. The developed framework is illustrated through specific flows in unstable regimes. In particular, we consider the flow behind a disk and the Rayleigh–Bénard convection, for which we construct bifurcation diagrams that describe the variation of the response as well as the energy transfers for different parameters associated with the considered flows. We reveal the low dimensionality of the underlying stochastic attractor.

Key words: low-dimensional models, nonlinear instability, turbulent transition

1. Introduction

The fluid flows encountered in realistic technological and natural settings are usually characterized by complexity and uncertainty in their form and dynamics. This complexity is expressed by the presence of multiple temporal and spatial scales on a single realization, the existence of multiple attractors (e.g. multiple steady states) and often the continuous transition of the system state between these different dynamical regimes. An effective framework for the global analysis of systems presenting such complexity is the probabilistic one, where, in the general case, the response is characterized not through a single realization but through a continuously infinite set of possible realizations accompanied with a probability measure that quantifies the likelihood of their occurrence. However, the efficient computation of those statistical

† Email address for correspondence: sapsis@mit.edu

responses remains a very challenging problem, since flows with the above features are usually connected with non-Gaussian statistics, strongly transient behaviour and spatially inhomogeneous features. Examples occur in fluid mechanics and turbulence (Monin & Yaglom 1971; Vincent & Meneguzzi 1991; Briscolini & Santangelo 1994; Jaberi *et al.* 1996; Li & Meneveau 2005), ocean and atmospheric dynamics (Schertzer & Lovejoy 1987; CPSMA 1993; Lermusiaux, Chiu & Robinson 2002; Auclair, Marsaleix & De Mey 2003; Dee & Da Silva 2003; Lermusiaux *et al.* 2006; Sura 2010), gravity waves (Jansen 2003) and magnetohydrodynamics (Marsch & Tu 1997), just to mention a few.

Various approaches have been developed for the characterization, description and quantification of uncertainty in these complex systems. A large class of those uncertainty quantification (UQ) methods rely on the assumption of *ad hoc* reduced-order dynamics (fixed in time) such as the proper orthogonal decomposition (POD) method (see e.g. Sirovich 1987; Berkooz, Holmes & Lumley 1993; Holmes, Lumley & Berkooz 1996). Improved variants of POD have also been developed based on linear-operator-theoretic model reduction methods, such as the balanced POD (Lall, Marsden & Glavaski 2002; Ma, Rowley & Tadmor 2010) and the bilateral coupling between variations in the fluctuation growth rate and the mean flow variations (Tadmor *et al.* 2010, 2011). In all of the above methods, however, the static character of the employed modes does not allow for an efficient set-up of a low-dimensional but adaptive reduced-order model that can reproduce important features of the original system such as strongly non-Gaussian statistics and transient instabilities.

A different approach is based on the closure of the stochastic problem by assuming specific statistical structure for the response. The simplest approach along this line is the Gaussian closure (Epstein 1969), a UQ scheme whose basic assumption is equivalent with zero nonlinear energy fluxes between dynamical components (see Sapsis & Majda (2013*c*) for an overview). Along the same spirit are the polynomial chaos (PC) method and its variants, with the main difference being that the projection is not performed over a Gaussian stochastic basis but rather on non-Gaussian elements that come from a given family of orthogonal polynomials. The PC method has been applied extensively in fluid flow analysis (Chorin 1974; Le Maitre *et al.* 2001; Xiu & Karniadakis 2003; Knio & Le Maitre 2006), and various of its limitations for intermittent instabilities have been discussed recently in Majda & Branicki (2012).

The purpose of this work is to develop and illustrate a new, efficient, non-Gaussian order-reduction approach for the UQ of complex flows characterized by low-dimensional stochastic attractors. The main tool that we will use will be a novel reduction technique based on the application of the dynamically orthogonal (DO) field equations (Sapsis & Lermusiaux 2009), a set of closed evolution equations that describe (compute) the time-dependent reduced-order space where stochasticity 'lives' as well as its spatio-temporal and non-Gaussian statistical characteristics. Using this theory and methodology, for specific initial condition probabilities or family of perturbations, we can provide a precise and global description of all the possible states that a flow can evolve into, as well as their relative probabilities. Additionally, we are able to characterize the flow of energy or probability between these states and their role on the chaotic character of the flow realizations that one obtains when the problem is solved deterministically. Of course, our results are linked to uncertainty quantification, but the present work is not concerned with the estimation of errors in model equations (Lermusiaux 2006; Branicki & Majda 2012) nor in the errors due to numerical discretization (e.g. Roache 1997).

The structure of the paper is as follows. In § 2 we present the DO field equations for the general case of a Boussinesq fluid in a three-dimensional domain in the presence of convection and rotation. Special emphasis is given to the treatment of the stochastic pressure that allows for significant reduction of the computational cost. We also discuss the case of stochastic boundary conditions and illustrate how to convert a problem of this kind into an equivalent one having deterministic boundary conditions and the stochastic part of the boundary conditions acting as interior forcing in the governing differential equations. Section 3 is devoted to the study of energy exchanges, in the form of variance, between the mean flow and the stochastic fluctuations, and among DO modal fluctuations. Specifically, we see that the (stochastic) energy transfers occur between the mean flow and the DO modes, but also among pairs and triads of DO modes. Additionally, dissipation acts on the mean flow but also locally on each mode. In § 4, we study some specific cases of two-dimensional flows presenting complex behaviour: the flow behind the cylinder and the Rayleigh–Bénard convection. Both of these flows may develop, depending on the flow parameters, numerous instabilities leading to stochastic attractors of equal dimensionality (Sapsis 2013). The statistical form of the solution of both configurations presents special interest, since it leads to finite-dimensional stochastic attractors with strongly non-Gaussian features. We provide bifurcation diagrams illustrating the transition to these dynamical regimes in the parameter space as well as the associated energy transfers between the modes and the mean flow.

2. Dynamically orthogonal Navier–Stokes and Boussinesq equations

In this section, we derive the DO equations for general Newtonian fluids, focusing on the Navier–Stokes and Boussinesq equations. Let $(\Omega, \mathscr{B}, \mathscr{P})$ be a probability space, with Ω being the sample space containing the set of elementary events $\omega \in \Omega$, $\mathscr{B}$ the σ-algebra associated with Ω, and $\mathscr{P}$ a probability measure. Let $\boldsymbol{x} \in D \subseteq \mathbb{R}^n$ denote the spatial coordinates and $t \in T$ the time. Then every measurable map of the form $\Phi(\boldsymbol{x}, t; \omega), \ \omega \in \Omega$, will define a random field. In applications, the most important cases are where $n = 2$ or 3 spatial dimensions; therefore, we will assume that $\boldsymbol{x} \in D \subseteq \mathbb{R}^n, \ n = 2, 3$. We define the mean value operator

$$\bar{\Phi}(\boldsymbol{x}, t) = E^{\omega}[\Phi(\boldsymbol{x}, t; \omega)] = \int_{\Omega} \Phi(\boldsymbol{x}, t; \omega) \, \mathrm{d}\mathscr{P}(\omega), \tag{2.1}$$

as well as the covariance operator

$$\boldsymbol{C}_{\Phi_1(\cdot,t;\omega)\Phi_2(\cdot,s;\omega)}(\boldsymbol{x}, \boldsymbol{y}) = E^{\omega}[(\Phi_1(\boldsymbol{x}, t; \omega) - \bar{\Phi}_1(\boldsymbol{x}, t))(\Phi_2(\boldsymbol{y}, s; \omega) - \bar{\Phi}_2(\boldsymbol{y}, s))^{\mathrm{T}}], \quad \boldsymbol{x}, \boldsymbol{y} \in D, \ t, s \in T. \tag{2.2}$$

In what follows, we will always assume that the stochastic fields involved are square integrable and the covariance operator is always finite. For every two random fields $\Phi_1(\boldsymbol{x}, t; \omega)$ and $\Phi_2(\boldsymbol{x}, t; \omega)$, we denote the spatial inner product as

$$\langle \Phi_1(\cdot, t; \omega), \Phi_2(\cdot, t; \omega) \rangle. \tag{2.3}$$

This notation is also used for sub-fields for the case of vector fields $\boldsymbol{\Phi}$ (e.g. multivariate state). For multivariate state vectors, a normalized (weighted) form of the inner product is defined, as exemplified in the main text.

In what follows, we will use Einstein's convention for summation, i.e. $\sum_i a_i b_i = a_i b_i$ except if the limits of summation need to be shown. A double index that is not summed up will be denoted as $a_{\bar{i}} b_{\bar{i}}$.

2.1. *DO representation*

Using a generalized form (each term is time-dependent and we do not assume Gaussian statistics) of the Karhunen–Loève expansion, we have that every random field $\Phi(\boldsymbol{x}, t; \omega)$ can be approximated arbitrarily well by a finite series of the form

$$\Phi(\boldsymbol{x}, t; \omega) = \bar{\Phi}(\boldsymbol{x}, t) + \sum_{i=1}^{s} Y_i(t; \omega)\Phi_i(\boldsymbol{x}, t), \quad \omega \in \Omega, \tag{2.4}$$

where s is a sufficiently large non-negative integer and the $Y_i(t; \omega)$ are s scalar random coefficients. We define the stochastic subspace $\boldsymbol{V}_S = \mathrm{span}\{\Phi_i(\boldsymbol{x}, t)\}_{i=1}^{s}$ as the linear space spanned by the s deterministic fields $\Phi_i(\boldsymbol{x}, t)$. This is the set of modes that describe where the dominant uncertainty exists at every time instant. Initially those modes can be chosen as POD modes.

Clearly, representation (2.4) with all quantities $(\bar{\Phi}(\boldsymbol{x}, t),\ \{\Phi_j(\boldsymbol{x}, t)\}_{j=1}^{s},\ \{Y_j(t; \omega)\}_{j=1}^{s})$ varying is redundant, and therefore we cannot derive independent equations from the stochastic partial differential equation (SPDE) describing their evolution. Hence, additional constraints are imposed in order to get a well-posed problem for the unknown quantities. As shown in Sapsis & Lermusiaux (2009), an appropriate constraint is the DO condition: the rate of change of the stochastic subspace is orthogonal to itself, expressed as

$$\frac{\mathrm{d}\boldsymbol{V}_S}{\mathrm{d}t} \perp \boldsymbol{V}_S \quad \Longleftrightarrow \quad \left\langle \frac{\partial \Phi_i(\cdot, t)}{\partial t}, \Phi_j(\cdot, t) \right\rangle = 0, \quad i = 1, \ldots, s,\ j = 1, \ldots, s. \tag{2.5}$$

Note that the DO condition implies the preservation of orthonormality for the basis $\{\Phi_j(\boldsymbol{x}, t)\}_{j=1}^{s}$ itself since

$$\frac{\partial}{\partial t}\langle \Phi_i(\cdot, t), \Phi_j(\cdot, t)\rangle = \left\langle \frac{\partial \Phi_i(\cdot, t)}{\partial t}, \Phi_j(\cdot, t) \right\rangle + \left\langle \frac{\partial \Phi_j(\cdot, t)}{\partial t}, \Phi_i(\cdot, t) \right\rangle = 0, \quad i = 1, \ldots, s,\ j = 1, \ldots, s. \tag{2.6}$$

Inserting the DO representation (2.4) into the original governing differential equations and using the DO condition (2.5), one can derive a set of independent, explicit equations for all the unknown quantities. Specifically, we reformulate the original SPDE to an s-dimensional stochastic differential equation for the random coefficients $Y_i(t; \omega)$ coupled with $s + 1$ deterministic partial differential equations (PDEs) for the fields $\bar{\Phi}(\boldsymbol{x}, t)$ and $\Phi_i(\boldsymbol{x}, t)$. These equations are derived in the next subsection and, as we will see, they are not based on any assumptions for the form of the stochastic coefficients or the basis $\Phi_i(\boldsymbol{x}, t)$. In the derivation of the DO equations, the main assumption is the dynamical orthogonality condition, which comes as a natural representation constraint without any loss of generality for the representation.

Note that the dimensionality of the representation, s, depends not only on the stochastic complexity of the response but also on the complexity of the nonlinear dynamics. In the context of fluids, the dimensionality of the subspace as well as adaptive criteria for its variation are discussed in Sapsis & Lermusiaux (2012). The issue of the DO dimensionality in connection with its limitations to specific dynamics (e.g. non-normal or strong nonlinear energy cascades) is discussed thoroughly in Sapsis & Majda (2013*a*), where a simple triad example is considered to illustrate the dynamical regimes where discrepancies will occur. For the present work, the parameters considered are chosen so that the solution can be adequately represented with a moderate number of DO modes.

In the next subsections we will formulate the DO equations for the stochastic Navier–Stokes and Boussinesq equations. For simple illustrations of the DO method in simple systems, as well as comparisons with other methods (e.g. polynomial chaos, or blended methods), we refer to Sapsis & Majda (2013*a*) (application of the DO method on a triad nonlinear model) and Choi, Sapsis & Karniadakis (2013) (application of the DO method on linear advection and Burger's wave equation).

2.2. *Stochastic Navier–Stokes and Boussinesq equations*

We consider the general case of a weakly compressible Newtonian fluid in a rotating frame of reference and under a Boussinesq approximation, i.e. we neglect the small density variations in the momentum equations and in the first law of thermodynamics, except in the buoyancy term and in the linearized equation of state. Rotation is assumed to have a component only in the vertical direction (e.g. for localized ocean motions on the Earth's surface, this is the beta-plane approximation). After some manipulations (whose details can vary with the application (e.g. Gebhart *et al.* 1988; Cushman-Roisin & Beckers 2010; Kundu, Cohen & Dowling 2012) – here we employ the form of Härtel, Meiburg & Necker (2000)), one obtains the following non-dimensional conservation of momentum, energy and mass for a three-dimensional fluid in a domain D in a rotating frame at frequency f:

$$\frac{\partial \boldsymbol{u}}{\partial t} = -\boldsymbol{\nabla} p + \frac{1}{\sqrt{Gr}}\Delta \boldsymbol{u} - \boldsymbol{u}\cdot\boldsymbol{\nabla}\boldsymbol{u} - f\hat{\boldsymbol{k}}\times\boldsymbol{u} - \rho\hat{\boldsymbol{k}} + \bar{\boldsymbol{\tau}}(\boldsymbol{x},t) + \tilde{\boldsymbol{\tau}}(\boldsymbol{x},t;\omega)$$
$$\equiv \mathscr{L}_{\boldsymbol{u}}[\Phi(\boldsymbol{x},t;\omega);\omega], \tag{2.7a}$$

$$\frac{\partial \rho}{\partial t} = \frac{1}{Sc\sqrt{Gr}}\Delta\rho - \boldsymbol{u}\cdot\boldsymbol{\nabla}\rho \equiv \mathscr{L}_{\rho}[\Phi(\boldsymbol{x},t;\omega);\omega] \tag{2.7b}$$

$$0 = \operatorname{div}\boldsymbol{u}. \tag{2.7c}$$

Here the Langevin notation is used, introducing stochastic forcing and allowing for stochastic initial and boundary conditions. The non-dimensional random field variables are: the flow velocity $\boldsymbol{u} = (u(\boldsymbol{x},t;\omega), v(\boldsymbol{x},t;\omega), w(\boldsymbol{x},t;\omega))$, the density $\rho(\boldsymbol{x},t;\omega)$ and the pressure $p(\boldsymbol{x},t;\omega)$. (The dimensional variables, denoted with a hat, have been non-dimensionalized using $\hat{t} = t\sqrt{\hat{h}/\hat{g}'}$, $\hat{\boldsymbol{x}} = \boldsymbol{x}\hat{h}$, $\hat{\boldsymbol{u}} = \boldsymbol{u}\sqrt{\hat{g}'\hat{h}}$ and $\hat{\rho} = \hat{\rho}_{min} + \rho(\hat{\rho}_{max} - \hat{\rho}_{min})$.) The non-dimensional space and time variables are $(\boldsymbol{x},t)$. The Grashof number $Gr = \hat{g}'\hat{h}^3/\hat{\nu}^2$ is the ratio of buoyancy forces to viscous forces, and the Schmidt number $Sc = \hat{\nu}/\hat{\kappa}$ the ratio of kinematic viscosity $\hat{\nu}$ to molecular diffusivity $\hat{\kappa}$ for the density field, with $\hat{g}' = \hat{g}(\hat{\rho}_{max} - \hat{\rho}_{min})/\hat{\rho}_{avg}$ being the reduced gravity and $\hat{h}$ the vertical length scale. The non-dimensional Coriolis coefficient under the beta-plane approximation is $f = f_0 + \beta_0 y$ and $\hat{\boldsymbol{k}}$ is the unit vector in the z-direction. The state vector is given as $\Phi = (\boldsymbol{u},\rho)^{\mathrm{T}}$. At first order, the Boussinesq flow is incompressible. We note that the second prognostic equation for density originates from the thermodynamic energy equation and the linearized equation of state (it arises from another form of the Boussinesq approximation frequently used in ocean modelling, which retains the temperature and salinity fields as state variables (see e.g. Cushman-Roisin & Beckers 2010; Haley & Lermusiaux 2010)). If the density is constant, $\sqrt{Gr} \equiv Re$, that is, the square root of the Grashof number is replaced by the Reynolds number, and one recovers the incompressible form of the Navier–Stokes equations.

2.2.1. *Stochastic equations and forcing*

The solutions to (2.2.1) are random solution variables, driven by the statistics of the initial and boundary conditions as well as by stochastic forcing in the equations themselves. Here the latter are included only in the momentum equation, in the form of an external stress acting on the fluid: the vector $\bar{\boldsymbol{\tau}}(\boldsymbol{x}, t) = (\bar{\tau}_x(\boldsymbol{x}, t), \bar{\tau}_y(\boldsymbol{x}, t), \bar{\tau}_z(\boldsymbol{x}, t))$ is its external mean (deterministic) component and $\tilde{\boldsymbol{\tau}}(\boldsymbol{x}, t; \omega) = (\tilde{\tau}_x(\boldsymbol{x}, t; \omega), \tilde{\tau}_y(\boldsymbol{x}, t; \omega), \tilde{\tau}_z(\boldsymbol{x}, t; \omega))$ is its zero-mean stochastic component, for which we assume known the complete probabilistic information. To define this stochastic component, we consider its covariance operator

$$\boldsymbol{C}_{\tilde{\tau}\tilde{\tau}}(\boldsymbol{x}, \boldsymbol{y}) = E^{\omega}[\tilde{\boldsymbol{\tau}}(\boldsymbol{x}, t; \omega)\tilde{\boldsymbol{\tau}}(\boldsymbol{y}, t; \omega)^{\mathrm{T}}]. \tag{2.8}$$

We then diagonalize the probability measure associated with $\tilde{\boldsymbol{\tau}}(\boldsymbol{x}, t; \omega)$ by solving the following three-dimensional vector eigenvalue problem:

$$\int_D \boldsymbol{C}_{\tilde{\tau}\tilde{\tau}}(\boldsymbol{x}, \boldsymbol{y})\tilde{\boldsymbol{\tau}}_r(\boldsymbol{y}, t)\,\mathrm{d}\boldsymbol{y} = \lambda_r^2 \tilde{\boldsymbol{\tau}}_r(\boldsymbol{x}, t). \tag{2.9}$$

This provides the principal directions over which the probability measure is spread in the variance sense. Retaining only the first R terms, we obtain the following approximation of the stochastic field $\tilde{\boldsymbol{\tau}}(\boldsymbol{x}, t; \omega)$:

$$\tilde{\boldsymbol{\tau}}(\boldsymbol{x}, t; \omega) = \sum_{r=1}^{R} Z_r(t; \omega)\tilde{\boldsymbol{\tau}}_r(\boldsymbol{x}, t) = Z_r(t; \omega)\tilde{\boldsymbol{\tau}}_r(\boldsymbol{x}, t). \tag{2.10}$$

Here R is defined by the order of truncation of the full series, and $Z_r(t; \omega)$ are the stochastic forcing coefficients given by

$$Z_r(t; \omega) = \langle \tilde{\boldsymbol{\tau}}(\cdot, t; \omega), \tilde{\boldsymbol{\tau}}_r(\cdot, t) \rangle. \tag{2.11}$$

2.2.2. *Boundary and initial conditions*

We assume that the boundary conditions for the state Φ and for the pressure (if needed) are defined by the linear differential operator $\mathscr{B}$, i.e.

$$\mathscr{B}_{\Phi}[\Phi(\boldsymbol{\xi}, t; \omega)] = \bar{\Phi}_{\partial D}(\boldsymbol{\xi}, t), \quad \boldsymbol{\xi} \in \partial D, \tag{2.12a}$$

$$\mathscr{B}_{p}[p(\boldsymbol{\xi}, t; \omega)] = \bar{p}_{\partial D}(\boldsymbol{\xi}, t), \quad \boldsymbol{\xi} \in \partial D. \tag{2.12b}$$

The case of stochastic boundary conditions is discussed in the Appendix. We also assume that the initial conditions are stochastic with known statistics given by

$$\Phi(\boldsymbol{x}, t_0; \omega) = \Phi_0(\boldsymbol{x}; \omega), \quad \boldsymbol{x} \in D, \ \omega \in \Omega. \tag{2.13}$$

2.3. *Dynamically orthogonal equations*

Using the DO representation, i.e. a generalized Karhunen–Loève (KL) expansion, we now derive an exact set of dynamically orthogonal Navier–Stokes and Boussinesq equations that govern the evolution of the mean, modes and stochastic coefficients. The only approximation arises from the truncation of the DO representation to $s(t)$ terms. We first substitute the DO decomposition into the governing equations (2.2.1) to obtain:

$$\frac{\partial \bar{\boldsymbol{u}}}{\partial t} + \frac{\mathrm{d}Y_i}{\mathrm{d}t}\boldsymbol{u}_i + Y_i\frac{\partial \boldsymbol{u}_i}{\partial t} = \mathscr{L}_{\boldsymbol{u}}(\bar{\boldsymbol{u}} + Y_i\boldsymbol{u}_i, \bar{\rho} + Y_i\rho_i, p; \omega), \tag{2.14a}$$

$$\frac{\partial \bar{\rho}}{\partial t} + \frac{\mathrm{d}Y_i}{\mathrm{d}t}\rho_i + Y_i\frac{\partial \rho_i}{\partial t} = \mathscr{L}_{\rho}(\bar{\boldsymbol{u}} + Y_i\boldsymbol{u}_i, \bar{\rho} + Y_i\rho_i; \omega). \tag{2.14b}$$

It is from these equations (2.14) that we will derive the equations for the mean, modes and their coefficients, using the expectation operator, spatial inner product and DO condition. The spatial inner product for the multivariate state vector field Φ is defined by

$$\begin{aligned}\langle \Phi_1, \Phi_2 \rangle &= \langle \boldsymbol{u}_1, \boldsymbol{u}_2 \rangle + c_\rho \langle \rho_1, \rho_2 \rangle \\ &= \int_D (u_1 u_2 + v_1 v_2 + w_1 w_2 + c_\rho \rho_1 \rho_2)\, \mathrm{d}\boldsymbol{x}, \end{aligned} \tag{2.15}$$

where c_ρ is a positive coefficient. We note that there are several logical ways to select this constant and that there are also many possible inner-product choices. These are generic issues associated with reduction methods where some inner product or norm needs to be heuristically chosen. In this case we choose to define the inner product with respect to the velocity, since we are more interested in kinetic energy and larger spatial scales (in contrast to a vorticity formulation, where enstrophy and the smaller scales would be emphasized). Additionally, the constant c_ρ defines the relative importance between uncertainty of the density and the velocity field. Here we pick this constant so that the two fields involved have equally important contributions to the inner product and thus to the uncertainty quantification. Such an expected-variance normalization has been used successfully in many ocean applications (e.g. Lermusiaux 2006) and is logical based on our chosen KL decomposition (2.4).

2.3.1. *Stochastic dynamics operator*

We first expand the stochastic dynamics operator $\mathscr{L}$ in (2.14) to obtain

$$\begin{aligned}\mathscr{L}_{\boldsymbol{u}}[\Phi(\boldsymbol{x}, t; \omega); \omega] = &-\nabla p + \frac{1}{\sqrt{Gr}} \Delta \bar{\boldsymbol{u}} - \bar{\boldsymbol{u}} \cdot \nabla \bar{\boldsymbol{u}} - f \hat{\boldsymbol{k}} \times \bar{\boldsymbol{u}} - \bar{\rho} \hat{\boldsymbol{k}} + \bar{\boldsymbol{\tau}}(\boldsymbol{x}, t) \\ &+ Y_i \left[\frac{1}{\sqrt{Gr}} \Delta \boldsymbol{u}_i - \boldsymbol{u}_i \cdot \nabla \bar{\boldsymbol{u}} - \bar{\boldsymbol{u}} \cdot \nabla \boldsymbol{u}_i - f \hat{\boldsymbol{k}} \times \boldsymbol{u}_i - \rho_i \hat{\boldsymbol{k}} \right] \\ &- \frac{1}{2} Y_i Y_j [\boldsymbol{u}_i \cdot \nabla \boldsymbol{u}_j + \boldsymbol{u}_j \cdot \nabla \boldsymbol{u}_i] + Z_r(t; \omega) \tilde{\boldsymbol{\tau}}_r(\boldsymbol{x}, t), \end{aligned} \tag{2.16a}$$

$$\begin{aligned}\mathscr{L}_{\rho}[\Phi(\boldsymbol{x}, t; \omega); \omega] = &\frac{1}{Sc\sqrt{Gr}} \Delta \bar{\rho} - \bar{\boldsymbol{u}} \cdot \nabla \bar{\rho} \\ &+ Y_i \left[\frac{1}{Sc\sqrt{Gr}} \Delta \rho_i - \boldsymbol{u}_i \cdot \nabla \bar{\rho} - \bar{\boldsymbol{u}} \cdot \nabla \rho_i \right] \\ &- \frac{1}{2} Y_i Y_j [\boldsymbol{u}_i \cdot \nabla \rho_j + \boldsymbol{u}_j \cdot \nabla \rho_i]. \end{aligned} \tag{2.16b}$$

Moreover, by inserting the DO representation in the continuity equation, we obtain

$$\operatorname{div} \bar{\boldsymbol{u}} + Y_i(t; \omega) \operatorname{div} \boldsymbol{u}_i = 0. \tag{2.16c}$$

Since the last equation should hold for arbitrary $Y_i(t; \omega)$, we obtain the equivalent form

$$\operatorname{div} \bar{\boldsymbol{u}} = 0, \tag{2.16d}$$

$$\operatorname{div} \boldsymbol{u}_i = 0, \quad i = 1, \ldots, s. \tag{2.16e}$$

An important property of Navier–Stokes equations that allows for the efficient applicability of the DO method is the polynomial nonlinearities in the evolution operator $\mathscr{L}$. This form of the operator allows it to be expressed in a polynomial series that involves the unknown quantities of the DO representation (2.4). It is then possible

to derive closed evolution equations whose right-hand sides depend on finite-order moments of the stochastic coefficients, the DO modes and the mean field.

Note that, for the case of a non-polynomial or non-smooth operator $\mathscr{L}$, one would not be able to expand it into a polynomial series. The DO equations would still be applicable, but in general it would not be possible to compute their right-hand side efficiently using moments of the coefficients Y_i. In such a case, a change of variable or other transformations would be needed to remain efficient. If not, one would in general need moments of the full fields $\boldsymbol{\Phi}(\boldsymbol{x}, t; \omega)$, which, even though available, would involve significant computational cost.

2.3.2. *Stochastic pressure field*

To derive an equation for the pressure, we need to understand its role in the stochastic context of the operator $\mathscr{L}$ given above and DO representation. Pressure (for a Boussinesq or incompressible flow with a deterministic conservation of mass) is the stochastic quantity which guarantees that, for every possible realization ω, the evolved field $(u(\boldsymbol{x}, t; \omega), v(\boldsymbol{x}, t; \omega), w(\boldsymbol{x}, t; \omega))$ is divergence-free (take the divergence of the momentum equation (2.16*a*) and use the family of continuity equations to show this). Therefore, the stochastic pressure should be able to balance all the non-divergent contributions from the terms involved in the operator $\mathscr{L}$ (equation (2.16*a*)). To this end, we choose to represent the stochastic pressure field as

$$p = \bar{p} + Y_i(t; \omega) p_i - Y_i(t; \omega) Y_j(t; \omega) p_{ij} + Z_r(t; \omega) b_r. \tag{2.17}$$

Based on the above discussion, the mean pressure field components should satisfy the following equations:

$$\Delta \bar{p} = \operatorname{div}(-\bar{\boldsymbol{u}} \cdot \nabla \bar{\boldsymbol{u}} - f \hat{\boldsymbol{k}} \times \bar{\boldsymbol{u}} - \bar{\rho} \hat{\boldsymbol{k}} + \bar{\boldsymbol{\tau}}(\boldsymbol{x}, t)), \tag{2.18a}$$

$$\mathscr{B}_p[\bar{p}(\boldsymbol{\xi}, t)] = \bar{p}_{\partial D}(\boldsymbol{\xi}, t), \quad \boldsymbol{\xi} \in \partial D. \tag{2.18b}$$

The stochastic terms in $\mathscr{L}$ multiplied with $Y_i(t; \omega)$ will be balanced through the following equations:

$$\Delta p_i = \operatorname{div}(-\boldsymbol{u}_i \cdot \nabla \bar{\boldsymbol{u}} - \bar{\boldsymbol{u}} \cdot \nabla \boldsymbol{u}_i - f \hat{\boldsymbol{k}} \times \boldsymbol{u}_i - \rho_i \hat{\boldsymbol{k}}), \tag{2.18c}$$

$$\mathscr{B}_p[p_i(\boldsymbol{\xi}, t)] = 0, \quad \boldsymbol{\xi} \in \partial D, \ i = 1, \ldots, s. \tag{2.18d}$$

Similarly, for the stochastic terms multiplied by $Y_i(t; \omega) Y_j(t; \omega)$ we will have

$$\Delta p_{ij} = \tfrac{1}{2} \operatorname{div}(\boldsymbol{u}_i \cdot \nabla \boldsymbol{u}_j + \boldsymbol{u}_j \cdot \nabla \boldsymbol{u}_i), \tag{2.18e}$$

$$\mathscr{B}_p[p_{ij}(\boldsymbol{\xi}, t)] = 0, \quad \boldsymbol{\xi} \in \partial D, \ i, j = 1, \ldots, s. \tag{2.18f}$$

Finally, the forcing terms will be balanced through the family of equations:

$$\Delta b_r = \operatorname{div} \tilde{\boldsymbol{\tau}}_r(\boldsymbol{x}, t), \tag{2.18g}$$

$$\mathscr{B}_p[q_r(\boldsymbol{\xi}, t)] = 0, \quad \boldsymbol{\xi} \in \partial D, \ r = 1, \ldots, R. \tag{2.18h}$$

The above set of equations guarantees that, for every realization ω, the evolved field $\boldsymbol{u}(\boldsymbol{x}, t; \omega)$ will be incompressible (in the Boussinesq sense).

2.3.3. *Evolution of the mean fields $\bar{\boldsymbol{u}}(\boldsymbol{x}, t)$ and $\bar{\rho}(\boldsymbol{x}, t)$*

Taking the expectation of the governing equations (2.14) using the expanded right-hand sides and continuity equations (2.3*c*,*d*), we obtain the set of deterministic PDEs

for the mean field:

$$\frac{\partial \bar{\boldsymbol{u}}}{\partial t} = -\nabla \bar{p} + \frac{1}{\sqrt{Gr}}\Delta \bar{\boldsymbol{u}} - \bar{\boldsymbol{u}} \cdot \nabla \bar{\boldsymbol{u}} - f\hat{\boldsymbol{k}} \times \bar{\boldsymbol{u}} - \bar{\rho}\hat{\boldsymbol{k}} + \bar{\boldsymbol{\tau}}(\boldsymbol{x}, t) - \boldsymbol{C}_{Y_i(t)Y_j(t)} \left[-\nabla p_{ij} + \frac{1}{2}\boldsymbol{u}_i \cdot \nabla \boldsymbol{u}_j + \frac{1}{2}\boldsymbol{u}_j \cdot \nabla \boldsymbol{u}_i \right], \tag{2.19a}$$

$$\frac{\partial \bar{\rho}}{\partial t} = \frac{1}{Sc\sqrt{Gr}}\Delta \bar{\rho} - \bar{\boldsymbol{u}} \cdot \nabla \bar{\rho} - \frac{1}{2}\boldsymbol{C}_{Y_i(t)Y_j(t)} \left[\boldsymbol{u}_i \cdot \nabla \rho_j + \boldsymbol{u}_j \cdot \nabla \rho_i \right], \tag{2.19b}$$

$$0 = \operatorname{div} \bar{\boldsymbol{u}}, \tag{2.19c}$$

where $\boldsymbol{C}_{Y_i(t)Y_j(t)} = E^{\omega}[Y_i(t)Y_j(t)]$ and the following boundary conditions hold:

$$\mathscr{B}_{\Phi}[\bar{\Phi}(\boldsymbol{\xi}, t)] = \bar{\Phi}_{\partial D}(\boldsymbol{\xi}, t), \quad \boldsymbol{\xi} \in \partial D. \tag{2.20}$$

2.3.4. *Evolution of the stochastic subspace basis* $\boldsymbol{u}_i(\boldsymbol{x}, t)$, $\rho_i(\boldsymbol{x}, t)$

If we multiply the governing equations (2.14) with the stochastic coefficients Y_j, then apply the expectation operator and use the DO condition as well as the governing equations for the stochastic coefficients, we obtain the equations for the stochastic subspace basis (i.e. DO modes):

$$\frac{\partial \boldsymbol{u}_i}{\partial t} = \boldsymbol{Q}_{\boldsymbol{u},i} - [\langle \boldsymbol{Q}_{\boldsymbol{u},i}, \boldsymbol{u}_m \rangle + c_{\rho}\langle Q_{\rho,i}, \rho_m \rangle]\boldsymbol{u}_m, \tag{2.21a}$$

$$\frac{\partial \rho_i}{\partial t} = Q_{\rho,i} - [\langle \boldsymbol{Q}_{\boldsymbol{u},i}, \boldsymbol{u}_m \rangle + c_{\rho}\langle Q_{\rho,i}, \rho_m \rangle]\rho_m, \tag{2.21b}$$

$$0 = \operatorname{div} \boldsymbol{u}_i. \tag{2.21c}$$

Here

$$\begin{aligned} \boldsymbol{Q}_{\boldsymbol{u},i} &\equiv \boldsymbol{C}^{-1}_{Y_i(t)Y_j(t)} E^{\omega}[\mathscr{L}_{\boldsymbol{u}}[\Phi(\boldsymbol{x}, t; \omega); \omega] Y_j(t; \omega)] \\ &= -\nabla p_i + \frac{1}{\sqrt{Gr}}\Delta \boldsymbol{u}_i - \boldsymbol{u}_i \cdot \nabla \bar{\boldsymbol{u}} - \bar{\boldsymbol{u}} \cdot \nabla \boldsymbol{u}_i - f\hat{\boldsymbol{k}} \times \boldsymbol{u}_i - \rho_i \hat{\boldsymbol{k}} \\ &\quad - \boldsymbol{C}^{-1}_{Y_i(t)Y_j(t)} \boldsymbol{M}_{Y_j(t)Y_m(t)Y_n(t)} \left[-\nabla p_{mn} + \frac{1}{2}\boldsymbol{u}_m \cdot \nabla \boldsymbol{u}_n + \frac{1}{2}\boldsymbol{u}_n \cdot \nabla \boldsymbol{u}_m \right] \\ &\quad + \boldsymbol{C}^{-1}_{Y_i(t)Y_j(t)} \boldsymbol{C}_{Y_j(t)Z_r(t)} [-\nabla b_r + \tilde{\boldsymbol{\tau}}_r(\boldsymbol{x}, t)], \end{aligned} \tag{2.22}$$

with $\boldsymbol{M}_{Y_j(t)Y_m(t)Y_n(t)} = E^{\omega}[Y_j(t)Y_m(t)Y_n(t)]$ and

$$\begin{aligned} Q_{\rho,i} &\equiv \boldsymbol{C}^{-1}_{Y_i(t)Y_j(t)} E^{\omega}[\mathscr{L}_{\rho}[\Phi(\boldsymbol{x}, t; \omega); \omega] Y_j(t; \omega)] \\ &= \frac{1}{Sc\sqrt{Gr}}\Delta \rho_i - \boldsymbol{u}_i \cdot \nabla \bar{\rho} - \bar{\boldsymbol{u}} \cdot \nabla \rho_i \\ &\quad - \frac{1}{2}\boldsymbol{C}^{-1}_{Y_i(t)Y_j(t)} \boldsymbol{M}_{Y_j(t)Y_m(t)Y_n(t)} [\boldsymbol{u}_m \cdot \nabla \rho_n + \boldsymbol{u}_n \cdot \nabla \rho_m]. \end{aligned} \tag{2.23}$$

Moreover, we will have the following boundary conditions:

$$\mathscr{B}_{\Phi}[\Phi_i(\boldsymbol{\xi}, t)] = 0, \quad \boldsymbol{\xi} \in \partial D. \tag{2.24}$$

2.3.5. *Evolution of the stochastic coefficients* $Y_i(t; \omega)$

The set of evolution equations for the stochastic coefficients is obtained by projecting the governing equations (2.14) onto each mode i, applying the DO condition

and ensuring that each coefficient is of zero mean. The result takes the form of coupled stochastic differential equations (SDEs):

$$\frac{\mathrm{d}Y_i}{\mathrm{d}t} = A_{im}(t)Y_m + B_{imn}(t)Y_mY_n + D_i(t;\omega), \tag{2.25}$$

where

$$A_{im}(t) = \left\langle -\nabla p_m + \frac{1}{\sqrt{Gr}}\Delta \boldsymbol{u}_m - \boldsymbol{u}_m\cdot\nabla\bar{\boldsymbol{u}} - \bar{\boldsymbol{u}}\cdot\nabla\boldsymbol{u}_m - f\hat{\boldsymbol{k}}\times\boldsymbol{u}_m - \rho_m\hat{\boldsymbol{k}}, \boldsymbol{u}_i\right\rangle + c_\rho\left\langle \frac{1}{Sc\sqrt{Gr}}\Delta\rho_m - \boldsymbol{u}_m\cdot\nabla\bar{\rho} - \bar{\boldsymbol{u}}\cdot\nabla\rho_m, \rho_i\right\rangle, \tag{2.26a}$$

$$B_{imn}(t) = -\left\langle -\nabla p_{mn} + \frac{1}{2}\boldsymbol{u}_m\cdot\nabla\boldsymbol{u}_n + \frac{1}{2}\boldsymbol{u}_n\cdot\nabla\boldsymbol{u}_m, \boldsymbol{u}_i\right\rangle - c_\rho\frac{1}{2}\left\langle \boldsymbol{u}_m\cdot\nabla\rho_n + \boldsymbol{u}_n\cdot\nabla\rho_m, \rho_i\right\rangle, \tag{2.26b}$$

$$D_i(t;\omega) = -B_{imn}(t)\boldsymbol{C}_{Y_m(t)Y_n(t)} + \langle -\nabla b_r + \tilde{\boldsymbol{\tau}}_r(\boldsymbol{x},t), \boldsymbol{u}_i\rangle\, Z_r(t;\omega). \tag{2.26c}$$

2.3.6. *Efficient pseudo-stochastic pressures*

We now show that, for common pressure boundary conditions, the number of unknown stochastic pressures in (2.17) can be reduced to $s+1$ by defining adequate pseudo-stochastic pressures. Using § 2.3.1, we first note that each velocity DO mode only needs a single scalar field to enforce the continuity constraint. Inspecting (2.19) and (2.21), we therefore define new pseudo-stochastic pressures, which are a combination of the mean, linear and quadratic modal pressures:

$$\bar{p}' = \bar{p} - \boldsymbol{C}_{Y_iY_j}p_{ij}, \tag{2.27a}$$

$$p_i' = p_i - \boldsymbol{C}^{-1}_{Y_iY_j}\boldsymbol{M}_{Y_jY_mY_n}p_{mn} + \boldsymbol{C}^{-1}_{Y_iY_j}\boldsymbol{C}_{Y_jZ_r}\,b_r. \tag{2.27b}$$

With this definition, the quadratic modal pressures are eliminated from (2.19)–(2.21). However, substituting the pseudo-pressures into (2.25), we find that the right-hand side of (2.25) still retains terms of the form $\langle\nabla p_{mn}, \boldsymbol{u}_i\rangle$, which are projections of the quadratic stochastic pressure terms in the subspace. At first, this would indicate that the quadratic modal pressures are still needed, but for commonly used boundary conditions, the projections cancel, i.e. the inner products $\langle\nabla p_{mn}, \boldsymbol{u}_i\rangle$ are zero. To show this, we use the following form of the Gauss theorem (Zorich 2004). For every scalar field α and every divergence-free vector field $\boldsymbol{F}$, we have

$$\int_D \nabla\alpha(\boldsymbol{x})\cdot\boldsymbol{F}(\boldsymbol{x})\,\mathrm{d}\boldsymbol{x} = \int_{\partial D}\alpha(\boldsymbol{\xi})\boldsymbol{F}(\boldsymbol{\xi})\cdot\boldsymbol{n}(\boldsymbol{\xi})\,\mathrm{d}\boldsymbol{\xi}. \tag{2.28}$$

In particular, we have $\int_{\mathscr{D}}\nabla p_{mn}\cdot\boldsymbol{u}_i\,\mathrm{d}\mathscr{D} = \int_{\partial D}p_{mn}\boldsymbol{u}_i\cdot\boldsymbol{n}\,\mathrm{d}\boldsymbol{\xi}$. In many cases of interest, the boundary integral vanishes for classic pressure conditions along the domain boundaries. That is, for Dirichlet conditions on the mean velocity and Neumann conditions on the mean pressure (e.g. for wall conditions), we have zero conditions on the velocity modes and zero Neumann conditions on the pressure modes. For Dirichlet conditions on the mean pressures and Neumann conditions on the mean velocities (e.g. for an outlet), we have zero conditions on the pressure modes and zero Neumann conditions on the velocity modes. Because of this property, the quadratic stochastic pressure term in (2.25) can be dropped without any penalty. Thus, by defining new pseudo-stochastic pressures, we have shown that we reduce the number of stochastic pressure unknowns

from $s^2 + s + 1$ to $s + 1$. We note that, if pseudo-pressure is used: (i) all quadratic stochastic pressures can be recovered by solving the Poisson equations given in § 2.3.2; and (ii) even though it is not necessary to have the three equalities

$$\langle \nabla p_{mn}, \boldsymbol{u}_i \rangle = \langle \nabla p_m, \boldsymbol{u}_i \rangle = \langle \nabla b_r, \boldsymbol{u}_i \rangle = 0, \tag{2.29}$$

they will hold for the above classic boundary conditions, in which case the right-hand sides of the evolution equations for the stochastic coefficients can be obtained using the simpler forms

$$A_{im}(t) = \left\langle \frac{1}{\sqrt{Gr}} \Delta \boldsymbol{u}_m - \boldsymbol{u}_m \cdot \nabla \bar{\boldsymbol{u}} - \bar{\boldsymbol{u}} \cdot \nabla \boldsymbol{u}_m - f \hat{\boldsymbol{k}} \times \boldsymbol{u}_m - \rho_m \hat{\boldsymbol{k}}, \boldsymbol{u}_i \right\rangle + c_\rho \left\langle \frac{1}{Sc\sqrt{Gr}} \Delta \rho_m - \boldsymbol{u}_m \cdot \nabla \bar{\rho} - \bar{\boldsymbol{u}} \cdot \nabla \rho_m, \rho_i \right\rangle, \tag{2.30a}$$

$$B_{imn}(t) = -\frac{1}{2} \langle \boldsymbol{u}_m \cdot \nabla \boldsymbol{u}_n + \boldsymbol{u}_n \cdot \nabla \boldsymbol{u}_m, \boldsymbol{u}_i \rangle - c_\rho \frac{1}{2} \langle \boldsymbol{u}_m \cdot \nabla \rho_n + \boldsymbol{u}_n \cdot \nabla \rho_m, \rho_i \rangle, \tag{2.30b}$$

$$D_i(t; \omega) = -B_{imn}(t) \boldsymbol{C}_{Y_m(t) Y_n(t)} + \langle \tilde{\boldsymbol{\tau}}_r(\boldsymbol{x}, t), \boldsymbol{u}_i \rangle Z_r(t; \omega). \tag{2.30c}$$

2.3.7. *Summary of Navier–Stokes DO equations*

We emphasize that property (2.29) allows the integration of the evolving DO fields without computing the s^2 quadratic pressures at each time step. In particular, it allows efficient application of projection methods (Guermond, Minev & Shen 2006) for the numerical solution of the DO form of stochastic Navier–Stokes and Boussinesq equations (Ueckermann, Lermusiaux & Sapsis 2013).

To summarize, the Navier–Stokes DO equations that we solve in this paper consist of:

(i) the mean-field equation, with the stochastic pseudo-pressure defined previously

$$\frac{\partial \bar{\boldsymbol{u}}}{\partial t} = -\nabla \bar{p}' + \frac{1}{\sqrt{Gr}} \Delta \bar{\boldsymbol{u}} - \bar{\boldsymbol{u}} \cdot \nabla \bar{\boldsymbol{u}} - f \hat{\boldsymbol{k}} \times \bar{\boldsymbol{u}} - \bar{\rho} \hat{\boldsymbol{k}} + \bar{\boldsymbol{\tau}}(\boldsymbol{x}, t) - \boldsymbol{C}_{Y_i(t) Y_j(t)} \left[\frac{1}{2} \boldsymbol{u}_i \cdot \nabla \boldsymbol{u}_j + \frac{1}{2} \boldsymbol{u}_j \cdot \nabla \boldsymbol{u}_i \right], \tag{2.31}$$

$$\frac{\partial \bar{\rho}}{\partial t} = \frac{1}{Sc\sqrt{Gr}} \Delta \bar{\rho} - \bar{\boldsymbol{u}} \cdot \nabla \bar{\rho} - \frac{1}{2} \boldsymbol{C}_{Y_i(t) Y_j(t)} [\boldsymbol{u}_i \cdot \nabla \rho_j + \boldsymbol{u}_j \cdot \nabla \rho_i], \tag{2.32}$$

$$0 = \operatorname{div} \bar{\boldsymbol{u}}; \tag{2.33}$$

(ii) the equations for the basis given by (2.21), with an updated $\boldsymbol{Q}_{\boldsymbol{u},i}$ given by (written in terms of the pseudo-pressure)

$$\boldsymbol{Q}_{\boldsymbol{u},i} = -\nabla p_i' + \frac{1}{\sqrt{Gr}} \Delta \boldsymbol{u}_i - \boldsymbol{u}_i \cdot \nabla \bar{\boldsymbol{u}} - \bar{\boldsymbol{u}} \cdot \nabla \boldsymbol{u}_i - f \hat{\boldsymbol{k}} \times \boldsymbol{u}_i - \rho_i \hat{\boldsymbol{k}} - \boldsymbol{C}^{-1}_{Y_i(t) Y_j(t)} \boldsymbol{M}_{Y_j(t) Y_m(t) Y_n(t)} \left[\frac{1}{2} \boldsymbol{u}_m \cdot \nabla \boldsymbol{u}_n + \frac{1}{2} \boldsymbol{u}_n \cdot \nabla \boldsymbol{u}_m \right] + \boldsymbol{C}^{-1}_{Y_i(t) Y_j(t)} \boldsymbol{C}_{Y_j(t) Z_r(t)} \tilde{\boldsymbol{\tau}}_r(\boldsymbol{x}, t); \tag{2.34}$$

(iii) the stochastic ODE (2.29) with its coefficients given by (2.30*a*)–(2.30*c*).

For the solution of the coupled PDEs, we employ a conservative second-order finite-volume scheme in physical space with new advection schemes based on total variation diminishing methods. For the stochastic coefficients, we use time-marching

schemes of first to fourth order. The details of the numerical scheme employed as well as its convergence properties are presented in Ueckermann *et al.* (2013).

3. Stochastic energy exchanges

In this section we study energy exchange properties (in the sense of variance) between different DO modes and the mean flow. By construction, the DO modes always remain orthogonal, and this spatial orthogonality implies orthogonality of their spatial Fourier, Gabor and wavelet transforms (Daubechies 1992; Antoine *et al.* 2004). Therefore, different DO modes contain different frequency–phase content at the same spatial locations. The scope of this section is to derive closed expressions for the rate of energy or variance transfer from a given mode to the mean flow and to the other DO modes. These energy transfer rates, also known as model energy productions, have been studied previously in the deterministic context (see Rempfer & Fasel 1994; Noack *et al.* 2003). Here we will use a probabilistic framework to prove that this stochastic energy exchange among different modes and the mean flow occurs in both a linear and a nonlinear fashion, since the employed decomposition allows us to separate these two mechanisms. The second, nonlinear, mechanism is directly connected with the non-Gaussian statistics of the system state and it is also responsible for the triple interaction of DO modes.

To illustrate these properties, we consider a system with deterministic Dirichlet boundary conditions and zero stochastic and mean forcing. This set-up is sufficient to derive expressions for the stochastic energy transfer rates between different modes and the mean flow. Thus we set

$$\bar{\boldsymbol{\tau}}(\boldsymbol{x}, t) = \tilde{\boldsymbol{\tau}}(\boldsymbol{x}, t; \omega) = 0, \quad \boldsymbol{x} \in D, \ \omega \in \Omega, \tag{3.1}$$

$$\mathscr{B}_{\Phi}[\Phi_i(\boldsymbol{\xi}, t)] = 0, \quad \boldsymbol{\xi} \in \partial D. \tag{3.2}$$

3.1. *Energy exchanges I: general formulation*

We begin our analysis by presenting results on energy exchanges for the generic system (2.2.1) that models the dynamics of both the velocity field and the density/temperature field. In the next section we will consider the special case of an isothermal system.

3.1.1. *Stochastic energy exchanges between the principal DO modes and the mean*

To study the flow of stochastic energy (variance) among the mean flow and the DO modes, we consider the DO equation (2.25) for the stochastic coefficient $Y_i(t; \omega)$, since the fields $\boldsymbol{u}_i(\boldsymbol{x}, t)$ remain normalized. We assume that at the current time instant the covariance matrix $\boldsymbol{C}_{Y_m(t)Y_i(t)}$ has been diagonalized: in this way we have variance on the diagonal components only and the DO modes are time-evolving principal directions of the stochastic subspace (i.e. they take the form of a non-Gaussian KL expansion that has uncorrelated coefficients).

The goal is to study the transfer of energy from the mean flow to each principal mode i. Multiplying (2.25) with Y_i and applying the mean value operator, we obtain

$$\frac{1}{2}\frac{\mathrm{d}}{\mathrm{d}t}E^{\omega}[Y_i^2] = A_{ii}(t)E^{\omega}[Y_i^2] + B_{imn}(t)E^{\omega}[Y_i Y_m Y_n], \tag{3.3}$$

$$A_{ii}(t) = \left\langle \frac{1}{\sqrt{Gr}}\Delta \boldsymbol{u}_i - \boldsymbol{u}_i \cdot \nabla \bar{\boldsymbol{u}} - \bar{\boldsymbol{u}} \cdot \nabla \boldsymbol{u}_i - f\hat{\boldsymbol{k}} \times \boldsymbol{u}_i - \rho_i \hat{\boldsymbol{k}}, \boldsymbol{u}_i \right\rangle$$

$$+ c_{\rho} \left\langle \frac{1}{Sc\sqrt{Gr}}\Delta \rho_i - \boldsymbol{u}_i \cdot \nabla \bar{\rho} - \bar{\boldsymbol{u}} \cdot \nabla \rho_i, \rho_i \right\rangle, \tag{3.4a}$$

$$B_{imn}(t) = -\frac{1}{2}\langle \boldsymbol{u}_m \cdot \nabla \boldsymbol{u}_n + \boldsymbol{u}_n \cdot \nabla \boldsymbol{u}_m, \boldsymbol{u}_i\rangle - c_\rho \frac{1}{2}\langle \boldsymbol{u}_m \cdot \nabla \rho_n + \boldsymbol{u}_n \cdot \nabla \rho_m, \rho_i\rangle. \quad (3.4b)$$

We have

$$\langle \bar{\boldsymbol{u}} \cdot \nabla \boldsymbol{u}_i, \boldsymbol{u}_i\rangle + c_\rho \langle \bar{\boldsymbol{u}} \cdot \nabla \rho_i, \rho_i\rangle = \langle \bar{\boldsymbol{u}}, \nabla \mathscr{E}_i\rangle = 0, \quad (3.5)$$

where we have defined the field $\mathscr{E}_i = (\boldsymbol{u}_i^2 + c_\rho \rho_i^2)/2$, and the last equation follows from the Gauss theorem,

$$\langle \bar{\boldsymbol{u}}, \nabla \mathscr{E}_i\rangle = -\langle \operatorname{div} \bar{\boldsymbol{u}}, \mathscr{E}_i\rangle + \int_{\partial D} \mathscr{E}_i(\boldsymbol{\xi}, t)\bar{\boldsymbol{u}}(\boldsymbol{\xi}, t) \cdot \boldsymbol{n}(\boldsymbol{\xi})\, \mathrm{d}\boldsymbol{\xi}, \quad (3.6)$$

and the chosen deterministic boundary conditions, which lead to $\int_{\partial D} \mathscr{E}_i(\boldsymbol{\xi}, t)\bar{\boldsymbol{u}}(\boldsymbol{\xi}, t) \cdot \boldsymbol{n}(\boldsymbol{\xi})\, \mathrm{d}\,\boldsymbol{\xi} = 0$. Additionally, we have

$$\langle f\hat{\boldsymbol{k}} \times \boldsymbol{u}_i, \boldsymbol{u}_i\rangle = 0 \quad (3.7)$$

and, from the Gauss theorem and chosen boundary conditions,

$$\langle \Delta \boldsymbol{u}_i, \boldsymbol{u}_i\rangle = -\langle \nabla \boldsymbol{u}_i, \nabla \boldsymbol{u}_i\rangle, \quad (3.8a)$$

$$\langle \Delta \rho_i, \rho_i\rangle = -\langle \nabla \rho_i, \nabla \rho_i\rangle. \quad (3.8b)$$

Finally, we observe that

$$\langle \boldsymbol{u}_i \cdot \nabla \bar{\boldsymbol{u}}, \boldsymbol{u}_i\rangle = \int_D \boldsymbol{u}_i^{\mathrm{T}} \boldsymbol{S}_{\bar{\boldsymbol{u}}} \boldsymbol{u}_i\, \mathrm{d}\boldsymbol{x}, \quad (3.9)$$

where $\{\boldsymbol{S}_{\bar{\boldsymbol{u}}}\}_{ij} = (\partial \bar{u}_i/\partial x_j + \partial \bar{u}_j/\partial x_i)/2$. Overall, we thus obtain

$$\begin{aligned}\frac{1}{2}\frac{\mathrm{d}}{\mathrm{d}t}E^\omega[Y_i^2] = -\Bigg[&\frac{1}{\sqrt{Gr}}\langle \nabla \boldsymbol{u}_i, \nabla \boldsymbol{u}_i\rangle + c_\rho \frac{1}{Sc\sqrt{Gr}}\langle \nabla \rho_i, \nabla \rho_i\rangle \\ &+ \int_D \boldsymbol{u}_i^{\mathrm{T}} \boldsymbol{S}_{\bar{\boldsymbol{u}}} \boldsymbol{u}_i\, \mathrm{d}\boldsymbol{x} + \langle \rho_i \hat{\boldsymbol{k}}, \boldsymbol{u}_i\rangle + c_\rho \langle \boldsymbol{u}_i \cdot \nabla \bar{\rho}, \rho_i\rangle\Bigg] E^\omega[Y_i^2] \\ &- \frac{1}{2}[\langle \boldsymbol{u}_m \cdot \nabla \boldsymbol{u}_n + \boldsymbol{u}_n \cdot \nabla \boldsymbol{u}_m, \boldsymbol{u}_i\rangle \\ &+ c_\rho \langle \boldsymbol{u}_m \cdot \nabla \rho_n + \boldsymbol{u}_n \cdot \nabla \rho_m, \rho_i\rangle] E^\omega[Y_i Y_m Y_n]. \end{aligned} \quad (3.10)$$

We first observe that mean stochastic energy transfer between the stochastic mode i and the mean flow occurs in a linear way, although the terms in the original equation that are responsible for this energy transfer are the nonlinear ones (it is the quadratic terms in Navier–Stokes that lead to the terms $\boldsymbol{u}_i^{\mathrm{T}} \boldsymbol{S}_{\bar{\boldsymbol{u}}} \boldsymbol{u}_i$ and $\langle \boldsymbol{u}_i \cdot \nabla \bar{\rho}, \rho_i\rangle$ in (3.10)). Hence, for the dissipation due to fluid viscosity and density diffusion we have

$$\varepsilon_{diss,i} = -E^\omega[Y_i^2]\left[\frac{1}{\sqrt{Gr}}\langle \nabla \boldsymbol{u}_i, \nabla \boldsymbol{u}_i\rangle + c_\rho \frac{1}{Sc\sqrt{Gr}}\langle \nabla \rho_i, \nabla \rho_i\rangle\right], \quad (3.11)$$

and for the rate of energy transferred to or from the mean flow to mode i in the form of stochastic energy (variance) we have

$$\varepsilon_{mean \to i} = -E^\omega[Y_i^2]\left[\int_D \boldsymbol{u}_i^{\mathrm{T}} \boldsymbol{S}_{\bar{\boldsymbol{u}}} \boldsymbol{u}_i\, \mathrm{d}\boldsymbol{x} + c_\rho \langle \boldsymbol{u}_i \cdot \nabla \bar{\rho}, \rho_i\rangle\right]. \quad (3.12)$$

We also have a term associated with the transformation of kinetic to potential energy,

$$\varepsilon_{pot \leftrightarrow kin,i} = -E^\omega[Y_i^2]\langle \rho_i \hat{\boldsymbol{k}}, \boldsymbol{u}_i\rangle. \quad (3.13)$$

For small stochastic energy amplitudes $E^\omega[Y_i^2]$ (so that terms of $\mathcal{O}(Y^3)$ can be omitted), these three terms are those that mainly characterize the total energy variation of the mode $\boldsymbol{u}_i$, i.e. the total rate of energy change is given by

$$\varepsilon_{linear,i} \equiv \varepsilon_{diss,i} + \varepsilon_{mean\to i} + \varepsilon_{pot\leftrightarrow kin,i}. \tag{3.14}$$

In conclusion, in the absence of external source of stochasticity (i.e. when stochasticity is introduced only through the initial conditions), uncertainties are always reduced by dissipation and diffusion, but they are either amplified or tapered by the nonlinear stretching of the mean flow as well as the gradient of the mean density field, while exchanges between potential and kinetic forms of stochastic energy occur.

3.1.2. *Stochastic energy exchanges between the principal DO modes*

To study amplitude exchanges among various DO modes, we consider (3.10) just derived above. By inspection, we observe that the rate of energy transferred to mode i from all the DO modes is given by

$$\varepsilon_{DO\to i} = -\tfrac{1}{2}[\langle \boldsymbol{u}_m\cdot\nabla\boldsymbol{u}_n + \boldsymbol{u}_n\cdot\nabla\boldsymbol{u}_m, \boldsymbol{u}_i\rangle + c_\rho\langle \boldsymbol{u}_m\cdot\nabla\rho_n + \boldsymbol{u}_n\cdot\nabla\rho_m, \rho_i\rangle]E^\omega[Y_iY_mY_n]. \tag{3.15}$$

Since we had assumed that the modal covariance matrix $\boldsymbol{C}_{Y_m(t)Y_i(t)}$ had been diagonalized, the direct interactions of a pair of modes has been projected out. Such terms would correspond to dyadic exchanges of stochastic energy within the DO subspace, including conserved exchanges and internal growth or decay. Without these dyadic transfers, we consider that principal DO modes and stochastic energy transfers among these principal DO modes depend on the non-Gaussian characteristics of the probability measure (for Gaussian variables, we always have $E^\omega[Y_iY_mY_n] = 0$ and the triad term vanishes). Note that the $m = n = i$ term vanishes since, as for (3.5),

$$\langle \boldsymbol{u}_i\cdot\nabla\boldsymbol{u}_i, \boldsymbol{u}_i\rangle + c_\rho\langle \boldsymbol{u}_i\cdot\nabla\rho_i, \rho_i\rangle = \langle \boldsymbol{u}_i, \nabla\mathscr{E}_i\rangle = 0. \tag{3.16}$$

Hence, based on the above, we can have two types of interactions for these principal modes.

3.2. *Energy exchanges II: isothermal case*

To simplify technical details, we consider for now incompressible flows only, i.e. we derive expressions for the rate of energy transfer to a specific principal mode in the absence of density fluctuations. In the first type of principal mode interactions, we have interactions of two modes, say q and i, in a 'two–one triad' fashion, i.e. the distinct cases are $(m = q,\ n = i\ )$, or $(m = i,\ n = q)$, or $(n = m = q)$. For that type of 'two–one triad' interaction, summing all non-zero contributions, we obtain the rate of energy transferred between mode q and i:

$$\begin{aligned}
\varepsilon_{q\to i} &= -\langle \boldsymbol{u}_q\cdot\nabla\boldsymbol{u}_i + \boldsymbol{u}_i\cdot\nabla\boldsymbol{u}_q, \boldsymbol{u}_i\rangle E^\omega[Y_i^2Y_q] - \tfrac{1}{2}\langle \boldsymbol{u}_q\cdot\nabla\boldsymbol{u}_q + \boldsymbol{u}_q\cdot\nabla\boldsymbol{u}_q, \boldsymbol{u}_i\rangle E^\omega[Y_q^2Y_i]\\
&= -[\langle \boldsymbol{u}_i\cdot\nabla\boldsymbol{u}_q, \boldsymbol{u}_i\rangle + \langle \boldsymbol{u}_q\cdot\nabla\boldsymbol{u}_i, \boldsymbol{u}_i\rangle]E^\omega[Y_i^2Y_q] - \langle \boldsymbol{u}_q\cdot\nabla\boldsymbol{u}_q, \boldsymbol{u}_i\rangle E^\omega[Y_q^2Y_i]\\
&= -[\langle \boldsymbol{u}_i\cdot\nabla\boldsymbol{u}_q, \boldsymbol{u}_i\rangle + \tfrac{1}{2}\langle \boldsymbol{u}_q, \nabla|\boldsymbol{u}_i|^2\rangle]E^\omega[Y_i^2Y_q] - \langle \boldsymbol{u}_q\cdot\nabla\boldsymbol{u}_q, \boldsymbol{u}_i\rangle E^\omega[Y_q^2Y_i]\\
&= -\langle \boldsymbol{u}_i\cdot\nabla\boldsymbol{u}_q, \boldsymbol{u}_i\rangle E^\omega[Y_i^2Y_q] + \langle \boldsymbol{u}_q\cdot\nabla\boldsymbol{u}_i, \boldsymbol{u}_q\rangle E^\omega[Y_q^2Y_i]\\
&= -E^\omega[Y_i^2Y_q]\int_D \boldsymbol{u}_i^{\mathrm{T}}\boldsymbol{S}_{\boldsymbol{u}_q}\boldsymbol{u}_i\,\mathrm{d}\boldsymbol{x} + E^\omega[Y_q^2Y_i]\int_D \boldsymbol{u}_q^{\mathrm{T}}\boldsymbol{S}_{\boldsymbol{u}_i}\boldsymbol{u}_q\,\mathrm{d}\boldsymbol{x}.
\end{aligned} \tag{3.17}$$

In the above, we have used the assumed zero boundary conditions for the modes and the equality $\langle \boldsymbol{u}_q\cdot\nabla\boldsymbol{u}_q, \boldsymbol{u}_i\rangle = -\langle \boldsymbol{u}_q\cdot\nabla\boldsymbol{u}_i, \boldsymbol{u}_q\rangle$, which follows from direct application of the Gauss theorem. The two terms correspond to stretching of principal mode i

projecting onto principal mode q and the contracting of principal mode q projecting onto principal mode i.

The second type of principal mode interactions involves the interaction of modes in triads, where the energy transferred to mode i is due to its triad interaction with another pair of DO modes, e.g. modes p and q. The rate of energy transfer due to this truly triad interaction has the form

$$\begin{aligned}
\varepsilon_{pq\to i} &= -\tfrac{1}{2}\langle \boldsymbol{u}_p \cdot \nabla \boldsymbol{u}_q + \boldsymbol{u}_q \cdot \nabla \boldsymbol{u}_p, \boldsymbol{u}_i\rangle E^\omega[Y_i Y_p Y_q] \\
&= -\tfrac{1}{2}[\langle \boldsymbol{u}_q \cdot \nabla \boldsymbol{u}_p, \boldsymbol{u}_i\rangle + \langle \boldsymbol{u}_p \cdot \nabla \boldsymbol{u}_q, \boldsymbol{u}_i\rangle] E^\omega[Y_i Y_p Y_q] \\
&= \tfrac{1}{2}[\langle \boldsymbol{u}_q \cdot \nabla \boldsymbol{u}_i, \boldsymbol{u}_p\rangle + \langle \boldsymbol{u}_p \cdot \nabla \boldsymbol{u}_i, \boldsymbol{u}_q\rangle] E^\omega[Y_i Y_p Y_q] \\
&= \frac{1}{2}\left(\int_D \boldsymbol{u}_q^{\mathrm{T}} \boldsymbol{S}_{\boldsymbol{u}_i} \boldsymbol{u}_p \,\mathrm{d}\boldsymbol{x} + \int_D \boldsymbol{u}_p^{\mathrm{T}} \boldsymbol{S}_{\boldsymbol{u}_i} \boldsymbol{u}_q \,\mathrm{d}\boldsymbol{x}\right) E^\omega[Y_i Y_p Y_q] \\
&= \int_D \boldsymbol{u}_q^{\mathrm{T}} \boldsymbol{S}_{\boldsymbol{u}_i} \boldsymbol{u}_p \,\mathrm{d}\boldsymbol{x}\, E^\omega[Y_i Y_p Y_q]. \qquad (3.18)
\end{aligned}$$

Hence, this term corresponds to the stretching of principal mode direction i that projects on two other principal modes p and q.

We have derived expressions characterizing the transfer of mean energy to uncertainty (transfer of energy from the mean to the principal modes) but also the variance exchanges between principal modes. Motivated by these results, we define the following form of stochastic energy, where the energy of the mean and variance of the modes are considered in a unified way. As above, we restrict ourselves to incompressible Navier–Stokes flows and global kinetic energy only,

$$\begin{aligned}
\mathscr{E}_S &= \frac{1}{2} E^\omega[\langle \boldsymbol{u}, \boldsymbol{u}\rangle] = \frac{1}{2} E^\omega[\langle \bar{\boldsymbol{u}} + Y_i \boldsymbol{u}_i, \bar{\boldsymbol{u}} + Y_i \boldsymbol{u}_i\rangle] \\
&= \frac{1}{2}\left(\|\bar{\boldsymbol{u}}\|^2 + \sum_{i=1}^{s} E^\omega[Y_i^2]\right) \qquad (3.19)
\end{aligned}$$

where we have defined for convenience $\|\bar{\boldsymbol{u}}\|^2 = \langle \bar{\boldsymbol{u}}, \bar{\boldsymbol{u}}\rangle$. The next step is to study the evolution of the above quantity. We have, using the DO equations,

$$\begin{aligned}
\frac{\mathrm{d}\mathscr{E}_S}{\mathrm{d}t} &= E^\omega[\langle \bar{\boldsymbol{u}}, \bar{\boldsymbol{u}}_t\rangle] + E^\omega\left[Y_i \frac{\mathrm{d}Y_i}{\mathrm{d}t}\right] \\
&= E^\omega[\langle \bar{\boldsymbol{u}}, E^\omega[\mathscr{L}_{\boldsymbol{u}}]\rangle] + E^\omega[Y_i \langle \mathscr{L}_{\boldsymbol{u}} - E^\omega[\mathscr{L}_{\boldsymbol{u}}], \boldsymbol{u}_i\rangle] \\
&= E^\omega[\langle \bar{\boldsymbol{u}}, E^\omega[\mathscr{L}_{\boldsymbol{u}}]\rangle] + E^\omega[Y_i \langle \mathscr{L}_{\boldsymbol{u}}, \boldsymbol{u}_i\rangle] \\
&= E^\omega[\langle \mathscr{L}_{\boldsymbol{u}}, \bar{\boldsymbol{u}}\rangle] + E^\omega[\langle \mathscr{L}_{\boldsymbol{u}}, Y_i \boldsymbol{u}_i\rangle] \\
&= E^\omega[\langle \mathscr{L}_{\boldsymbol{u}}, \bar{\boldsymbol{u}} + Y_i \boldsymbol{u}_i\rangle] \\
&= E^\omega[\langle \mathscr{L}_{\boldsymbol{u}}, \boldsymbol{u}\rangle], \qquad (3.20)
\end{aligned}$$

which is as expected (from the deterministic kinetic energy equation).

3.2.1. *Case of zero mean flow boundary conditions*

The above result can be further expanded in the special but common cases of: (i) zero stochastic and mean forcing (as was assumed all along in this section); and (ii) zero boundary conditions on the mean velocity along the whole domain boundaries.

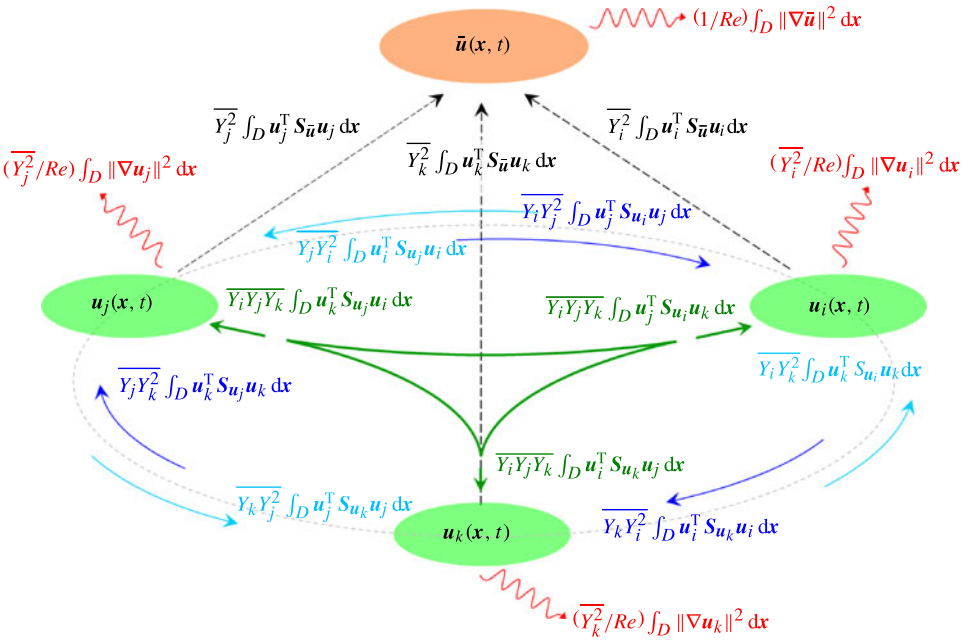

FIGURE 1. (Colour online) Energy exchanges between principal DO modes and the mean flow in stochastic, unforced, incompressible Navier–Stokes equations. The energy flow from the mean to the principal modes is characterized by the second-order statistics while variance exchange among the principal modes is characterized by the third-order statistics.

With these assumptions, the above result is expanded, using the Gauss theorem,

$$\begin{aligned}\frac{\mathrm{d}\mathscr{E}_S}{\mathrm{d}t} &= E^\omega[\langle\mathscr{L}_{\boldsymbol{u}},\boldsymbol{u}\rangle] = E^\omega\left[\left\langle\frac{1}{Re}\Delta\boldsymbol{u},\boldsymbol{u}\right\rangle\right]\\ &= -\frac{1}{Re}E^\omega[\langle\nabla\boldsymbol{u},\nabla\boldsymbol{u}\rangle]\\ &= -\frac{1}{Re}(\langle\nabla\bar{\boldsymbol{u}},\nabla\bar{\boldsymbol{u}}\rangle + E^\omega[Y_i^2]\langle\nabla\boldsymbol{u}_i,\nabla\boldsymbol{u}_i\rangle)\\ &= -\frac{1}{Re}(\|\nabla\bar{\boldsymbol{u}}\|^2 + E^\omega[Y_i^2]\|\nabla\boldsymbol{u}_i\|^2).\end{aligned} \tag{3.21}$$

Thus, the stochastic kinetic energy for incompressible Navier–Stokes flows (i) with null boundary conditions on the mean velocity and (ii) without stochastic and mean forcing, is dissipated due to viscosity, in full analogy with the usual notion of energy for deterministic Navier–Stokes. All the other forms of energy transfer from the mean flow to the DO modes and among the DO modes are internal system interactions. Of course, should the mean velocity boundary be non-zero somewhere along the boundaries or should a mean forcing be present in the interior, additional terms (i.e. pressure work, advection of kinetic energy and mean body/forcing work) will be present in this equation.

A summary of all the energy transfers in the incompressible unforced case is given in figure 1, where the internal interactions among the principal DO modes (green and blue arrows) are shown. The black arrows show the energy exchanges between

the mean flow and the principal modes. Finally, the red arrows represent the energy dissipation due to viscosity acting on both the mean flow and the principal modes.

4. Analysis of transient dynamics in fluid flows

We will now illustrate the use of the DO equations in the analysis of laminar flows with a small number of instabilities that lead to low-dimensional attractors of complex form (e.g. multiple steady states or effective dimensionality smaller than the reduced-order phase space dimensionality) and with strongly transient characteristics. Note that in this work the goal is to illustrate the applicability of the DO method in fluid flows with instabilities and to emphasize its importance in the analysis of energy transfers between dynamical components. To this end, we will only consider low-*Re* regimes where the number of instabilities is small – a feature that allows one to more easily describe nonlinear interactions and their role on the global dynamics.

Depending on the specific characteristics of the flow, the dynamics may possess a discrete or continuously infinite set of feasible states. The derived machinery allows for the determination of these states as well as the corresponding probability at which they occur. Additionally, the expressions for the energy rate transfer allows for the understanding of how these states are generated, e.g. where their energy is coming from. In what follows, we will consider two characteristic representatives of laminar flows with multiple states: flows behind a disk, as well as Rayleigh–Bénard flows. We will study the evolution of the statistical characteristics of these flows by initializing them with a very small stochastic perturbation with Gaussian statistics, and allow the internal instabilities of each flow to grow and give the multiple states that characterize the stochastic attractor at the given level of input energy.

4.1. *Flow behind a circular disk*

4.1.1. *Flow equations and geometry*

We consider viscous flows behind a circular disk; the same flows have been considered previously in Venturi, Wan & Karniadakis (2008) and Sapsis & Lermusiaux (2009) in the stochastic setting. Here we consider these flows again, but we seek to understand the energy transfer properties between the unstable mean and the dynamically evolving modes as well as their nonlinear interactions. As we will see, it is the interplay of linear instabilities and nonlinear energy transfers that allow energy to flow to linearly stable modes giving finite size to the attractor even along the linearly stable directions.

The governing equations for this case take the form

$$\frac{\partial \boldsymbol{u}}{\partial t} = -\nabla p + \frac{1}{Re}\Delta \boldsymbol{u} - \boldsymbol{u}\cdot\nabla\boldsymbol{u}, \tag{4.1}$$

$$0 = \operatorname{div}\boldsymbol{u}. \tag{4.2}$$

The geometry of the flow, together with the boundary conditions, is shown in figure 2. The diameter of the disk is $a = 1$ and it is located at a distance $d_1 = 4.5$ from the inlet of the flow. The length and width of the computational domain are 20×3 (non-dimensional) and the spatial resolution used is $N_x \times N_y = 400 \times 60$, while the time step used is $\delta t = 0.004$. The initial conditions consist of random perturbations with harmonic dependence in space and Gaussian stochastic structure (see Sapsis & Lermusiaux (2009) for details). The DO numerical scheme used is presented in full detail in Ueckermann *et al.* (2013). The Reynolds number of the flow is defined as $Re = Ua/\nu$, where ν is the kinematic viscosity. For the simulations that follow, we set $U = 1$ and $a = 1$, and thus $Re = \nu^{-1}$.

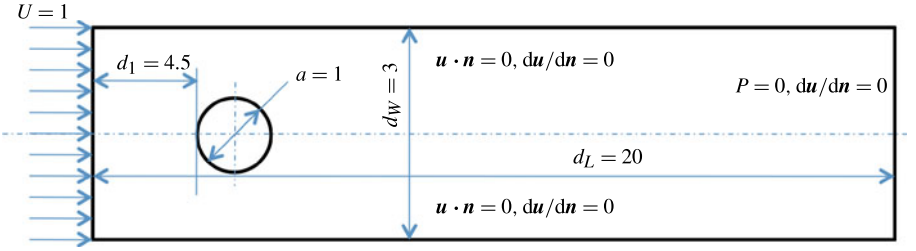

FIGURE 2. (Colour online) Sketch of the flow behind the circular disk.

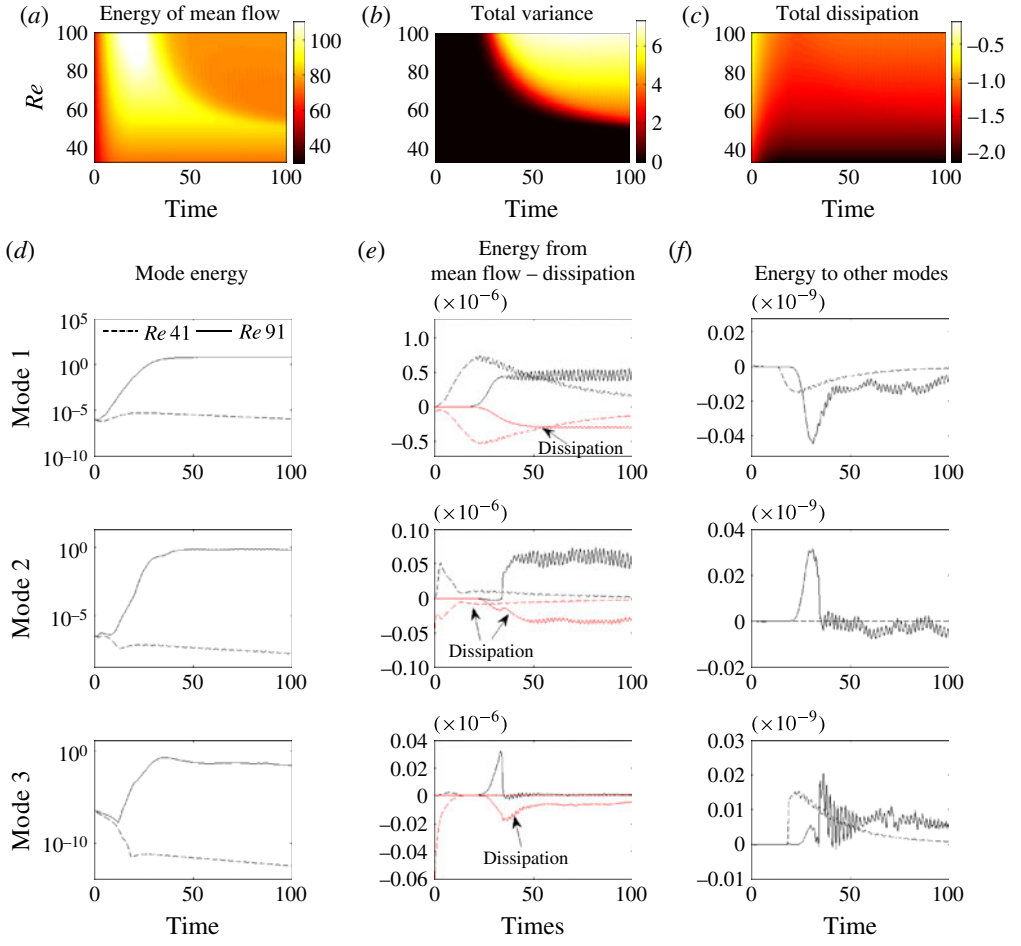

FIGURE 3. (Colour online) Top: energy of mean flow, total variance and total dissipation rate for the flow behind a disk over different *Re* numbers. Lower time-series plots: energy of the first three modes together with energy exchange rates between the mean and the other modes for two different *Re* numbers corresponding to stable and unstable dynamics.

4.1.2. *Stochastic response – stable regime and transitions*

In figure 3(*a*), we present the energy of the mean flow, the total variance as well as the total dissipation rate as functions of time and *Re* number. It is clear from the second plot that between $Re = 40$ and $Re = 50$ a bifurcation occurs, making the mean

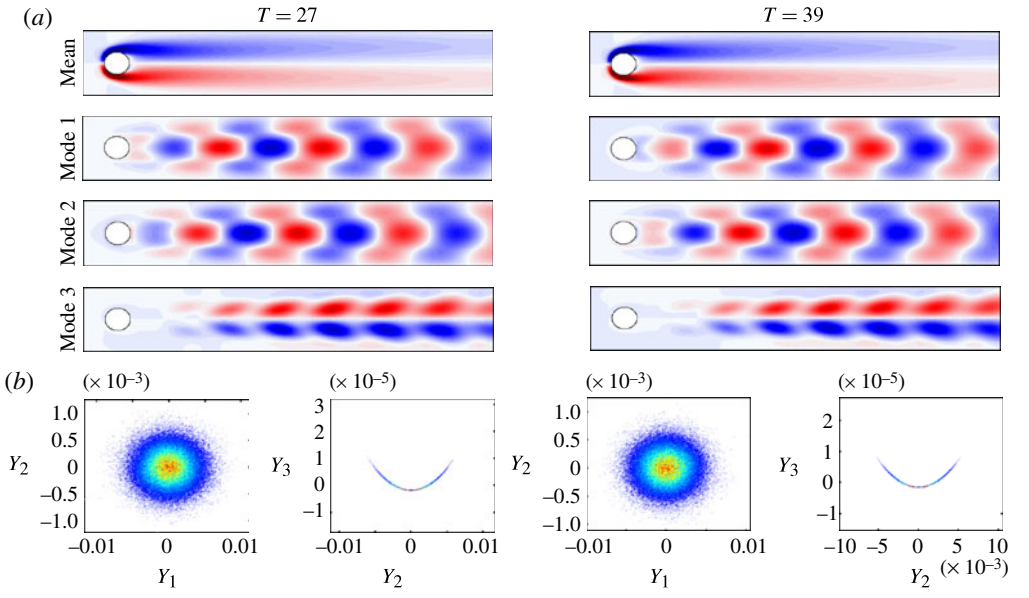

FIGURE 4. (Colour online) Mean flow and DO modes in terms of vorticity in the stable regime ($Re = 41$). The joint statistics are also presented for the first three modes (in the form of two-dimensional marginals for pairs of modes). The Gaussian statistics between the first two modes indicate their negligible energy interaction.

flow linearly unstable. The exact value of the transition is known to be $Re_c = 43$ and can be approximately obtained by the present analysis by integration of the reduced-order equations. This transition to instability is expressed through the variance growth of the DO modes that adaptively track and so reveal the unstable directions in phase space (see figure 5).

More specifically, we can observe from the plots that immediately after $t = 0$ the mean flow energy grows. Then depending on the Re number, this energy is either retained to the mean flow (stable regime) or it is transformed to variance of the DO modes (unstable regime). In figure 4 we present in more detail the mean field and DO modes for a stable Re number ($Re = 41$). We can observe that the first two modes are an oscillatory pair presenting spatially periodic structure that travels downstream – these two modes are strongly related since their spatial topology is shifted by half a temporal period and they essentially express a linearly stable oscillatory mode that corresponds to an eigenvalue with a non-zero imaginary part (Strouhal frequency). The DO scheme predicts that, after an initial transient growth, the energy of this spatially periodic perturbation (described by the first two modes) tends to decay, since the dissipation dominates the small positive value of energy transfer from the mean (dashed line, figure 3*e*). Concerning the statistical structure of the coefficients, we see that for the first two modes it is strongly Gaussian (figure 4) – a feature that indicates zero nonlinear energy transfers between modes 1 and 2 (see figure 1). Even though the third mode has non-Gaussian statistical connection with the first two modes, the energy of the latter is continuously decreasing (due to dissipation and energy flowing towards the mean), therefore not allowing for any important energy transfer to the third DO mode (figure 3*e*).

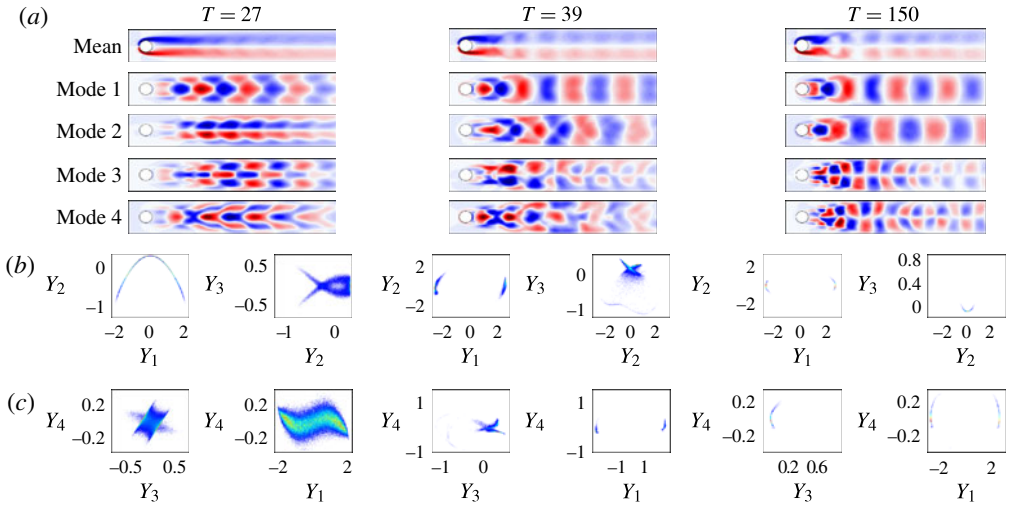

FIGURE 5. (Colour online) Stochastic response of the flow behind the disk in the unstable regime ($Re = 91$) for three different time instants. For each time, the mean flow and the DO modes are presented in terms of their vorticity together with the joint statistics of the first four stochastic coefficients.

4.1.3. *Stochastic response – unstable regime*

The situation is reversed in the unstable regime. To analyse this case, we consider a sufficiently large $Re = 91$. We can distinguish three different dynamical regimes. In the first phase of the dynamics ($t < 20$), the first two DO modes have exactly the same spatial structure as the DO modes of $Re = 41$, i.e. the spatially periodic structure that comes in pairs of shifted modes. However, in this case we have an exponential growth of their amplitude – during this dynamical regime the statistics of the two modes remain Gaussian and there is no significant energy transfer between those modes and other modes. Right after $t = 20$ a bifurcation occurs and the second DO mode becomes antisymmetric (see figure 5*a*) while the probability density function (p.d.f.) of the first two stochastic coefficients collapses into an effectively one-dimensional set (see p.d.f. plot for $T = 27$ in figure 5*b*). A detailed explanation of this collapse and its connection with the number of positive Lyapunov exponents or instabilities is given in Sapsis (2013), where it is rigorously proven that the effective dimensionality of the p.d.f. cannot exceed the number of instabilities or positive Lyapunov exponents. Here, this fact is illustrated, since we can directly observe that during the collapse of the $Y_1 - Y_2$ p.d.f. (after $t \sim 20$) there is only the first mode that is linearly unstable – for the second mode both dissipation and energy transfer from the mean are negative. The strongly non-Gaussian shape of the p.d.f. creates nonlinear energy transfer from the first to the second mode, as can be directly seen from figure 3(*f*). Thus, during this transitional phase, we have only one linearly unstable mode, the first one, which absorbs energy from the mean, and due to the non-Gaussian statistics passes some of this energy (the rest is dissipated) to the linearly stable modes. In this way, even though only one mode is linearly unstable, a series of stable modes have finite amount of energy – a detailed analysis of these energy transfer features and its implications in turbulent systems having a very large number of instabilities is given in Sapsis & Majda (2013*c*). These modes need to have non-Gaussian joint statistical structure with the linearly unstable modes in order for the nonlinear energy transfers to be activated.

After this transition phase (after $t = 40$), the flow enters a statistically stationary regime where the first two modes absorb energy from the mean flow through a complex pair of oscillatory modes (i.e. as happened during the initially transient instability). Both of these modes dissipate an important amount of this energy and the rest is sent to the third mode (note the negative values of mode-to-modes energy transfer in figure 3*f*). For the latter, we observe that the energy dissipation is much larger than the energy received from the mean flow. In this way, even though there are only two modes with positive Lyapunov exponents (i.e. the two modes for which the energy transfer from the mean is larger than dissipation), energy is spread along a much larger number of modes. Note that the fact that some of the energy is returned back to the mean does not contradict the common picture in fluid dynamics that energy eventually dissipates in small scales. The reason that we have energy flowing back to the mean here has to do with the fact that we are dealing with a low-dimensional attractor where the high-frequency modes still have sufficiently large scales so that their energy is not completely dissipated and exchanges with the mean still occur.

4.2. *Rayleigh–Bénard convection*

The second application that we consider is the Oberbeck–Boussinesq approximation to convection, which can lead to multiple steady-state regimes (Gelfgat, Bar-Yoseph & Yarin 1999) that are physically realizable (Pallares, Grau & Giralt 1999). The stochastic bifurcation properties for this flow have been studied in Venturi, Wan & Karniadakis (2010); here we are interested in performing a detailed uncertainty quantification analysis of both the transient and steady-state regimes. We first present the steady-state variance of the first and second DO modes for various Rayleigh and Prandtl numbers. Subsequently, we determine the various parametric domains that lead to qualitatively different results and present the details of the statistical responses and the associated stochastic attractors that give rise to multiple steady-state responses.

4.2.1. *Flow equations and geometry*

We consider the Navier–Stokes equations in the form (2.2.1) and we apply the rescaling

$$\boldsymbol{x} \to (Ra\,Pr)^{-1/6}\boldsymbol{x}, \quad t \to (Ra\,Pr)^{1/6}t, \tag{4.3}$$

$$\rho \to -(Ra\,Pr)^{1/2}T, \quad p \to (Ra\,Pr)^{-2/3}p, \tag{4.4}$$

where we use the non-dimensional numbers Ra and Pr (employed in the Oberbeck–Boussinesq approximation) given by

$$Gr\,Sc \Rightarrow Ra \quad \text{and} \quad Sc \Rightarrow Pr, \tag{4.5}$$

and we also use temperature T instead of density used in (2.2.1). After applying the above rescaling, we obtain the Oberbeck–Boussinesq approximation, which will be used for our analysis

$$\frac{\partial \boldsymbol{u}}{\partial t} = -\nabla p + Pr\,\Delta \boldsymbol{u} - \boldsymbol{u}\cdot\nabla\boldsymbol{u} + Ra\,Pr\,T\hat{\boldsymbol{k}}, \tag{4.6a}$$

$$\frac{\partial T}{\partial t} = \Delta T - \boldsymbol{u}\cdot\nabla T, \tag{4.6b}$$

$$0 = \operatorname{div}\boldsymbol{u}. \tag{4.6c}$$

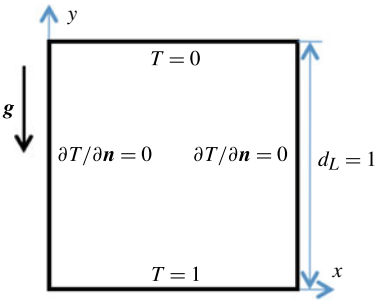

FIGURE 6. (Colour online) Sketch of the configuration for the Rayleigh–Bénard convection.

We consider non-dimensional numbers with order $Pr \sim 0.1$–1 and $Ra \sim 1.5 \times 10^4$–2×10^4 since for these values important bifurcations occur (Venturi *et al.* 2010). The geometry of the flow is assumed to be a square domain (figure 6) with $d_L = 1$ and with constant temperature on the top and bottom boundaries,

$$T = 1 \quad \text{for } y = 0, \tag{4.7a}$$

$$T = 0 \quad \text{for } y = 1, \tag{4.7b}$$

and homogeneous Neumann boundary conditions for the two vertical sides. Additionally, we assume no-slip boundary conditions for the velocity. We discretize the domain with an $N_x \times N_y = 64 \times 64$ grid and we use a time step $\delta t = 0.001$; the details of the DO numerical scheme are presented in Ueckermann *et al.* (2013).

To estimate the quantity c_ρ for the inner product, we estimate the magnitude of the field quantities. From the boundary conditions, we will have $T \sim \mathcal{O}(1)$. Moreover, since we are interested in performing UQ in the unstable regime, advection will be important, and thus we expect a scaling of the form $u^2/d_L \sim Ra\,Pr\,T$. This implies that $u \sim \mathcal{O}(10)$–$\mathcal{O}(100)$. Based on this scaling of the field quantities, we choose $c_\rho = 10$ (the equations we have considered are in non-dimensional form and so is c_ρ), so that both the temperature and the velocity play an equally important role in the inner product and thus in the evolution of the stochastic subspace. We emphasize that the results that we present in the sequel are robust with respect to the exact value of the parameter c_ρ as long as the stochastic dynamics remain consistent with the scaling argument we have just presented.

We initiate the mean flow using a superposition of the first two eigenfields of the linearized equation,

$$\bar{\boldsymbol{u}}_0 = \left(\frac{\partial \psi}{\partial y}, -\frac{\partial \psi}{\partial x} \right) \quad \text{with } \psi = 0.3X_1(x)Y_1(y) + 0.2X_2(x)Y_2(y), \tag{4.8a}$$

$$\bar{T}_0 = 1 - y, \tag{4.8b}$$

where the expressions for X_i and Y_i can be found in Venturi *et al.* (2010). We also apply a small, two-dimensional, stochastic perturbation in the temperature field with Gaussian statistics having variance $(\sigma_1^2, \sigma_2^2) = (10^{-1}, 10^{-5})$, and with spatial shape given by

$$T_{1,0} = 2\cos 8\pi x \cos \pi y, \tag{4.9a}$$

$$T_{2,0} = 2\cos \pi x \cos \pi y. \tag{4.9b}$$

4.2.2. *Deterministic response*

We first recall some properties of the deterministic dynamics and in particular some stability properties of the flow in the parametric regime we chose. A detailed bifurcation analysis is presented in Venturi *et al.* (2010). In this work the authors show that in the parametric regime we consider here there are two stable steady states coexisting: one characterized by a single rolling motion, and the other by a double rolling motion. The single roll has much higher energy than the double-roll motion. We emphasize that the linearly stable character of the above motions does not necessarily imply their existence in the stochastic response. In particular, their probability of occurrence depends on the domain of attraction, which is a nonlinear property of the system. Therefore, although linear stability analysis predicts the existence of both of these motions, we will see later that the domain of attraction for each one of them can lead to completely different probabilities of occurrence.

4.2.3. *Stochastic response*

We integrate the DO equations with two modes for long enough so that the system reaches a statistical steady state. The steady-state energy of the two modes with respect to the non-dimensional numbers Ra and Pr is shown in figure 7. There are two well-separated regions corresponding to the stochastically stable (zero variance or deterministic) and unstable behaviour. Both modes are active over the same parametric region – this is because, as we will see later, the second mode absorbs its energy directly from the first mode and not from the mean. The strength of the first mode, which corresponds to a single rolling motion of the fluid inside the square domain (see figure 8), shows a uniform dependence over the Ra number, while it increases monotonically with the Pr number until the bifurcation value, at which point the energy suddenly vanishes. On the other hand, the second mode (having a double symmetric roll structure) presents a more uniform dependence over the Pr number, while its energy increases as the Ra number increases until the stochastic stability boundary. We first discuss the character of the flow in the two different regimes (separated by the stochastic stability boundary).

In figure 8 we present the stochastic response of the flow for a set of parameters lying in the stable regime ($Ra = 18\,900$ and $Pr = 1.025$). In this case the mean has a double-roll symmetric structure while the first mode has an antisymmetric structure with a single dominant roll. The second mode consists of four rolls in a symmetric configuration. The non-Gaussian shape of the p.d.f. indicates that there is a nonlinear energy transfer of energy from mode 1 to mode 2. However, the linearly stable character of both modes does not allow for any growth of their energy and the deterministic mean flow dominates.

In contrast, for a set of parameters lying in the unstable regime ($Ra = 16\,050$ and $Pr = 0.45$), a small stochastic perturbation grows rapidly until it reaches the size of the stochastic attractor. In particular, as we can observe in figure 9, the mean flow retains its double-roll symmetric structure having also two smaller rolls forming in the bottom of the domain. The first mode retains the same topology with the stable regime, while the second mode now has a double-roll symmetric structure. The evolution of the p.d.f. also presents interesting features. In particular, the initially Gaussian shape is rapidly converging into a p.d.f. with effective dimensionality close to one, indicating a reduced-order dynamical system with one stable and one unstable direction (Sapsis 2013). The strongly non-Gaussian shape also reveals the important energy transfer from mode 1 to mode 2. As time evolves, more and more probability concentrates to the lobes of the p.d.f., gradually giving rise to a bimodal stochastic attractor consisting

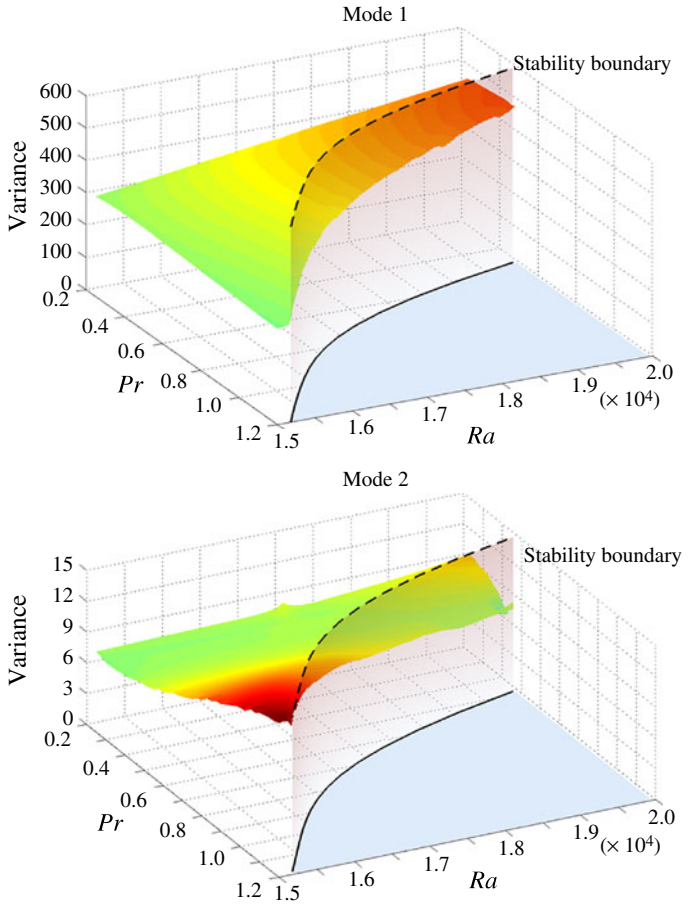

FIGURE 7. (Colour online) Variance of the two DO modes with respect to different Ra and Pr numbers for the Rayleigh–Bénard convection. The stability boundary separates the regions of finite-amplitude response. The shading/colour of the surfaces indicate the variance at this point (i.e. the vertical coordinate).

of two symmetric stages with a strong, positive and negative, rolling motion of the fluid and a weaker double-roll motion.

We emphasize that over the considered parametric regime the linear stability properties of the two motions remain invariant: both single and double roll are linearly stable equilibria. However, using stochastic analysis, we have revealed a stochastic stability boundary $Ra(Pr)$ over which the coexisting equilibrium points collapse to a robust double-roll motion with specific directionality. The robustness of this double rolling fluid motion, which takes place for large enough Ra numbers where forcing due to the temperature field is more intense, is probably related to the low energy of the corresponding stable equilibrium (see bifurcation analysis in Venturi *et al.* (2010)), which makes it easier to reach from an energetic point of view. On the other hand, in the stochastic regime, we have the coexistence of both single and double rolling motions, with the first one giving rise to the second one due to a secondary instability, which has been well documented here through the analysis of energy transfer properties.

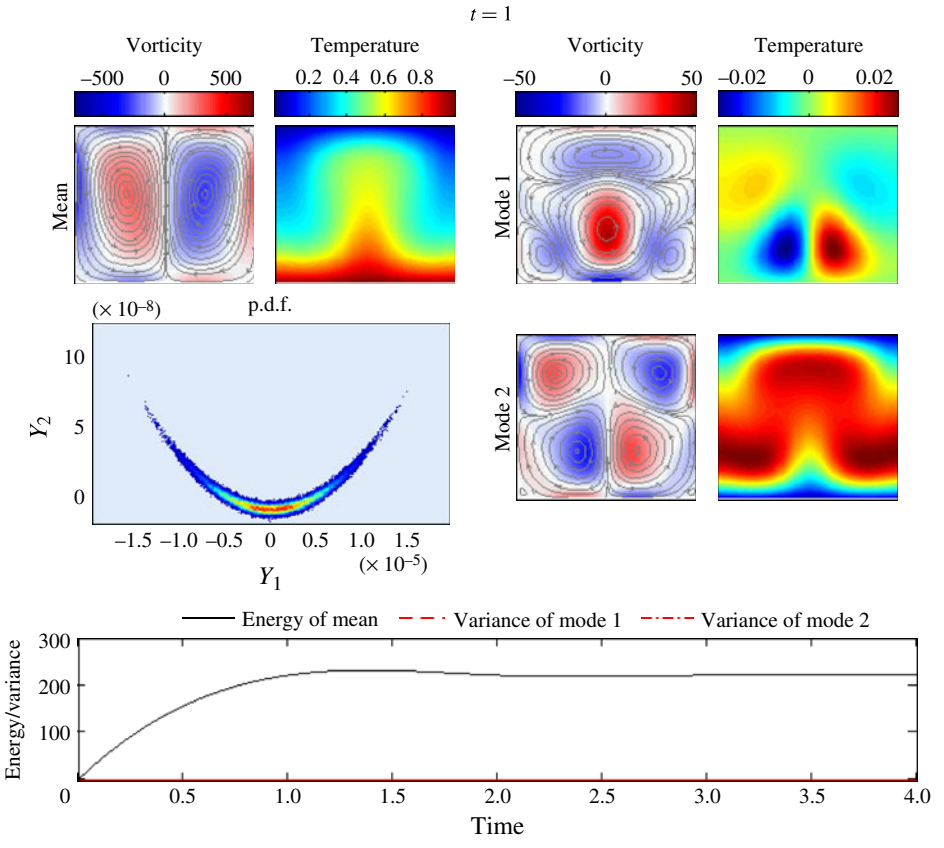

FIGURE 8. (Colour online) Stochastic response of the Rayleigh–Bénard convection in the stable regime ($Ra = 18\,900$ and $Pr = 1.025$). The mean vorticity and temperature field are presented together with modes 1 and 2. The joint p.d.f. is also presented together with the time series for the energies.

5. Conclusions

We have given a global characterization of the stochastic attractor and analysed the energy transfer properties in laminar fluid flows with internal instabilities. We have seen that these energy transfer properties are inherently connected with: (i) the linear instabilities of the mean flow; and (ii) the shape of the stochastic attractor and in particular with its non-Gaussian properties. In order to perform the above analysis, we have used the DO order-reduction framework, suitably formulated for Navier–Stokes and Boussinesq equations, which allows for efficient uncertainty quantification particularly for systems with low-dimensional attractors. The time-dependent character of the DO modes allows for the determination of a very efficient basis that can track the stochastic attractor more effectively especially during transient regimes.

To illustrate the energy transfer properties, we selected two laminar flows with a small number of internal instabilities, the flow behind a disk and the Rayleigh–Bénard convection. We first performed a bifurcation analysis to determine how the second-order properties vary with respect to the non-dimensional numbers involved. Subsequently, we focused on the different dynamical regimes and interpreted

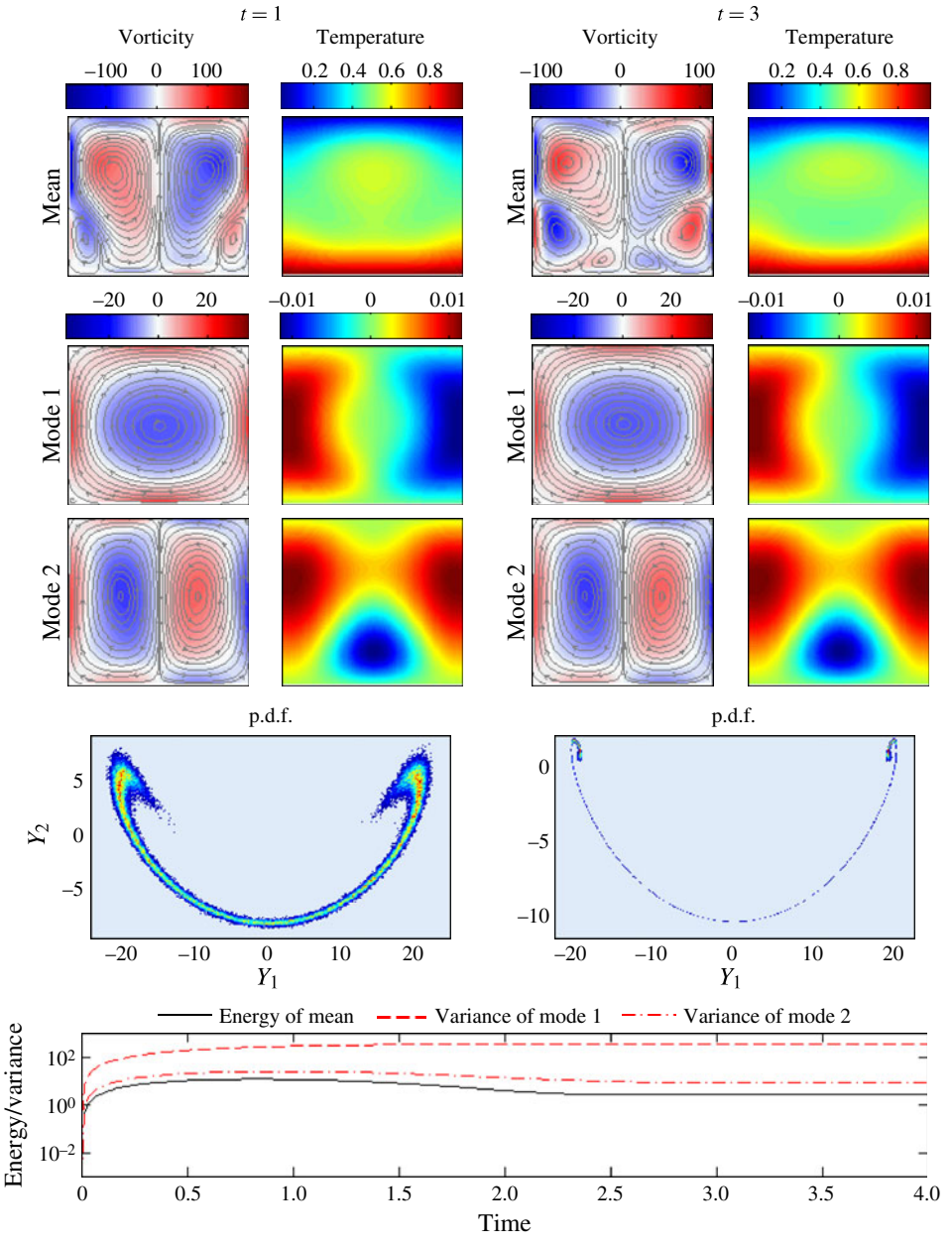

FIGURE 9. (Colour online) Stochastic response of the Rayleigh–Bénard convection in the unstable regime ($Ra = 16\,050$ and $Pr = 0.45$). The mean vorticity and temperature field are presented together with modes 1 and 2 for two different time instants. The joint p.d.f. is also presented together with the time series for the energies.

the stochastic response in terms of the energy transfer properties between the modes and the mean and between the modes themselves.

In contrast to the traditional linear stability and bifurcation analysis, the presented stochastic framework has the advantage of revealing inherently nonlinear properties of

the flow such as nonlinear energy transfers, domains of attraction for the various stable steady states and stochastic stability boundaries. There are properties of crucial importance since they are associated with the robustness and probability of occurrence of the dynamical modes of motion predicted by the deterministic analysis. A characteristic example is the Rayleigh–Bénard flow considered over a parametric regime where linear analysis predicts uniform dynamical properties while the actual stochastic attractor of the flow goes through an important bifurcation associated with secondary instabilities that give rise to nonlinear energy transfers and lead to the coexistence of two modes of fluid motion.

The present work also provides an important paradigm, illustrating the interplay between stochastic properties and global dynamical properties in fluid flows where order reduction is feasible; thus it covers a large spectrum of modern fluid dynamics applications and beyond. Extension into three-dimensional flows is feasible, although the computational cost associated with the coupled evolution of multiple three-dimensional flow fields may introduce technical challenges. Moreover, extension to non-laminar, turbulent flows requires the development of new UQ tools that can handle the essentially irreducible character of the dynamics while they can still be computationally tractable. In this way we should be able to handle problems of very high dimensionality (such as turbulence) and be able in this context to quantify the connection between energy transfers and stochastic characteristics; results along this direction will be reported in the near future (Sapsis & Majda 2013*c*,*b*).

Acknowledgements

We would like to thank the MSEAS group members for helpful discussions. We are grateful to the Office of Naval Research (ONR) for support under grants N00014-08-1-1097 (ONR6.1) and N00014-08-1-0586 (QPE) to the Massachusetts Institute of Technology (MIT). M.P.U. and P.F.J.L. also thank ONR for support under grants N00014-09-1-0676 (Science of Autonomy – A-MISSION) and N00014-12-1-0944 (ONR6.2) to MIT, as well as to the Natural Sciences and Engineering Research Council (NSERC) of Canada for partially supporting M.P.U. at MIT. We also thank the anonymous reviewers for their helpful suggestions.

Appendix. The case of stochastic boundary conditions

Here we consider the problem of stochastic boundary conditions and show how, under certain conditions, it can be transformed into stochastic forcing in the interior, i.e. an additional term in the governing equations. For simplicity, we assume that uncertainty is contained in the boundary velocity conditions only, although the results can be generalized. We assume that the complete stochastic information for the boundary conditions is known. More specifically, we have

$$\mathscr{B}_{\Phi}[\Phi(\boldsymbol{\xi},t;\omega)] = \bar{\Phi}_{\partial D}(\boldsymbol{\xi},t) + \Phi'_{\partial D}(\boldsymbol{\xi},t;\omega) = \bar{\Phi}_{\partial D}(\boldsymbol{\xi},t) + \begin{pmatrix} \boldsymbol{u}'_{\partial D}(\boldsymbol{\xi},t;\omega) \\ 0 \end{pmatrix}, \quad \boldsymbol{\xi} \in \partial D, \tag{A 1}$$

where $\Phi'_{\partial D}(\boldsymbol{\xi},t;\omega)$ is the zero-mean stochastic part of the boundary conditions. As for the initial conditions, we consider the covariance operator associated with the boundary conditions

$$\boldsymbol{C}_{\partial D\,\partial D}(\boldsymbol{\xi}_1,\boldsymbol{\xi}_2) = E^{\omega}[\boldsymbol{u}'_{\partial D}(\boldsymbol{\xi},t;\omega)\boldsymbol{u}'_{\partial D}(\boldsymbol{\xi},t;\omega)^{\mathrm{T}}]. \tag{A 2}$$

We formulate the eigenvalue problem to determine the principal directions along which the probability is distributed in the dominant variance sense:

$$\int_{\partial D} \boldsymbol{C}_{\partial D\,\partial D}(\boldsymbol{\xi}_1, \boldsymbol{\xi}_2)\boldsymbol{u}_{\partial D,k}(\boldsymbol{\xi}_2,t)\,\mathrm{d}\boldsymbol{\xi}_2 = \lambda_k^2 \boldsymbol{u}_{\partial D,k}(\boldsymbol{\xi}_1,t). \tag{A 3}$$

Using this information, we expand the stochastic boundary conditions as follows:

$$\mathscr{B}_{\Phi}[\Phi(\boldsymbol{\xi}, t; \omega)] = \bar{\Phi}_{\partial D}(\boldsymbol{\xi}, t) + \Xi_k(t; \omega) \begin{pmatrix} \boldsymbol{u}'_{\partial D,k}(\boldsymbol{\xi}, t) \\ 0 \end{pmatrix}, \quad \boldsymbol{\xi} \in \partial D, \tag{A 4}$$

where k is an index taking values from $1, \ldots, K$, the order of the truncation, and the stochastic coefficients are given by

$$\Xi_k(t; \omega) = \int_{\partial D} \boldsymbol{u}'_{\partial D}(\boldsymbol{\xi}, t; \omega)^{\mathrm{T}} \boldsymbol{u}_{\partial D,k}(\boldsymbol{\xi}, t)\,\mathrm{d}\boldsymbol{\xi}. \tag{A 5}$$

Assuming specific conditions on the above boundary forcing problem, we now transform it into an equivalent one having deterministic boundary conditions but with additional interior stochastic forcing. The idea is to handle the effect of stochastic boundary conditions through the partition of the solution into a component $\boldsymbol{\Phi}_h(\boldsymbol{x}, t; \omega) = (\boldsymbol{u}_h^{\mathrm{T}}, \rho_h)^{\mathrm{T}}$ that will satisfy the deterministic part of the boundary conditions, and a set of incompressible and irrotational components $\boldsymbol{u}_{b,k}(\boldsymbol{x}, t)$ that will satisfy the stochastic part of the boundary conditions. Specifically, we assume we can write the solution of the system at any given fixed time t as

$$\begin{pmatrix} \boldsymbol{u}(\boldsymbol{x}, t; \omega) \\ \rho(\boldsymbol{x}, t; \omega) \end{pmatrix} = \begin{pmatrix} \boldsymbol{u}_h(\boldsymbol{x}, t; \omega) \\ \rho_h(\boldsymbol{x}, t; \omega) \end{pmatrix} + \Xi_k(t; \omega) \begin{pmatrix} \boldsymbol{u}_{b,k}(\boldsymbol{x}, t) \\ 0 \end{pmatrix}. \tag{A 6}$$

Since the velocity fields $\boldsymbol{u}_{b,k}(\boldsymbol{x}, t)$ have been assumed irrotational and incompressible, there is a set of scalar potentials $\phi_{b,k}(\boldsymbol{x}, t)$ such that

$$\boldsymbol{u}_{b,k}(\boldsymbol{x}, t) = \nabla \phi_{b,k}(\boldsymbol{x}, t), \tag{A 7a}$$

$$\Delta \phi_{b,k}(\boldsymbol{x}, t) = 0. \tag{A 7b}$$

Moreover, each potential function $\phi_{b,k}(\boldsymbol{x}, t)$ will satisfy the following boundary conditions:

$$\mathscr{B}_{\Phi}\left[\begin{pmatrix} \nabla \phi_{b,k}(\boldsymbol{\xi}, t) \\ 0 \end{pmatrix}\right] = \begin{pmatrix} \boldsymbol{u}_{\partial D,k}(\boldsymbol{\xi}, t) \\ 0 \end{pmatrix}, \quad \boldsymbol{\xi} \in \partial D. \tag{A 8}$$

Note that time in the above elliptic equation acts as a parameter; thus there is no need for initial conditions. With the above choice, we have a well-defined problem for the potentials $\phi_{b,k}(\boldsymbol{x}, t)$ and additionally our solution satisfies the stochastic part of the boundary conditions. Moreover, we require $\boldsymbol{\Phi}_h(\boldsymbol{x}, t; \omega)$ to satisfy the deterministic part of the boundary conditions and in this way we obtain the following problem for $\boldsymbol{\Phi}_h(\boldsymbol{x}, t; \omega)$:

$$\begin{aligned} \frac{\partial \boldsymbol{\Phi}_h}{\partial t} = {} & \mathscr{L}\left[\boldsymbol{\Phi}_h(\boldsymbol{x}, t; \omega) + \Xi_k(t; \omega) \begin{pmatrix} \nabla \phi_{b,k}(\boldsymbol{x}, t) \\ 0 \end{pmatrix}; \omega\right] \\ & - \frac{\partial}{\partial t}\left(\Xi_k(t; \omega) \begin{pmatrix} \nabla \phi_{b,k}(\boldsymbol{x}, t) \\ 0 \end{pmatrix}\right), \end{aligned} \tag{A 9}$$

$$0 = \operatorname{div} \boldsymbol{u}_h, \tag{A 10}$$

with deterministic boundary conditions

$$\mathscr{B}_{\Phi}[\Phi_h(\boldsymbol{\xi}, t; \omega)] = \bar{\Phi}_{\partial D}(\boldsymbol{\xi}, t), \quad \boldsymbol{\xi} \in \partial D, \tag{A 11}$$

and initial conditions

$$\boldsymbol{\Phi}_h(\boldsymbol{x}, t_0; \omega) = \boldsymbol{\Phi}_0(\boldsymbol{x}; \omega) - \Xi_k(t_0; \omega) \begin{pmatrix} \nabla \phi_{b,k}(\boldsymbol{x}, t_0) \\ 0 \end{pmatrix}, \quad \boldsymbol{x} \in D, \ \omega \in \Omega. \tag{A 12}$$

Therefore, we have transformed the general problem to one with deterministic boundary conditions and interior stochastic forcing. We note that the following assumptions are required for the above to be efficient, including: (i) the K boundary forcing modes need to satisfy sufficient smoothness conditions; and (ii) the stochastic solution of the original Navier–Stokes or Boussinesq equations (forced by the stochastic boundary conditions) need to be well approximated by the stochastic solution of the transformed problem, which is forced by the truncated interior expansion defined by (A 7)–(A 8).

We note that handling the stochastic boundary conditions through the interior is of special importance for the case of systems where the initial state is deterministic and uncertainty is introduced only through the boundary conditions (i.e. the stochastic subspace is initially an empty set). In this case the DO modes required to describe the current state of the system may be very few compared to those required to satisfy the stochastic boundary conditions. Using the above decomposition, we create a new set of modes that depend exclusively on the stochastic characteristics of the boundary conditions and not on the system state. Hence, in this formulation the stochastic boundary conditions can be satisfied *a priori* (since we have solved for the potentials $\phi_{b,k}(\boldsymbol{\xi}, t)$) and we only need to solve for the uncertainty of the solution in the interior of the domain.

REFERENCES

ANTOINE, J. P., MURENZI, R., VANDERGHEYNST, P. & ALI, S. T. 2004 *Two-Dimensional Wavelets and Their Relatives*. Cambridge University Press.

AUCLAIR, F., MARSALEIX, P. & DE MEY, P. 2003 Space–time structure and dynamics of the forecast error in a coastal circulation model of the Gulf of Lions. *Dyn. Atmos. Oceans* **36**, 309–346.

BERKOOZ, G., HOLMES, P. & LUMLEY, J. 1993 The proper orthogonal decomposition in the analysis of turbulent flows. *Annu. Rev. Fluid Mech.* **25**, 539–575.

BRANICKI, M. & MAJDA, A. J. 2012 Quantifying uncertainty for predictions with model error in non-Gaussian systems with intermittency. *Nonlinearity* **25**, 2543–2578.

BRISCOLINI, M. & SANTANGELO, P. 1994 The non-Gaussian statistics of the velocity field in low-resolution large-eddy simulations of homogeneous turbulence. *J. Fluid Mech.* **270**, 199–218.

CHOI, M., SAPSIS, T. P. & KARNIADAKIS, G. E. 2013 A convergence study for SPDEs using combined polynomial chaos and dynamically-orthogonal schemes. *J. Comput. Phys.* **245**, 281–301.

CHORIN, A. J. 1974 Gaussian fields and random flow. *J. Fluid. Mech.* **85**, 325–347.

CPSMA, 1993 *Statistics and Physical Oceanography*. National Academies Press.

CUSHMAN-ROISIN, B. & BECKERS, J. M. 2010 *Introduction to Geophysical Fluid Dynamics. Physical and Numerical Aspects*. Academic Press.

DAUBECHIES, I. 1992 *Ten Lectures on Wavelets*. Society of Industrial and Applied Mathematics.

DEE, D. P. & DA SILVA, A. M. 2003 The choice of variable for atmospheric moisture analysis. *Mon. Weath. Rev.* **131**, 155–171.

EPSTEIN, E. S. 1969 Stochastic dynamic predictions. *Tellus* **21**, 739–759.

GEBHART, B., JALURIA, Y., MAHAJAN, R. L. & SAMMAKIA, B. 1988 *Buoyancy-Induced Flows and Transport*. Taylor and Francis.

GELFGAT, A., BAR-YOSEPH, P. Z. & YARIN, A. L. 1999 Stability of multiple steady states of convection in laterally heated cavities. *J. Fluid Mech.* **338**, 315–334.

GUERMOND, J. L., MINEV, P. & SHEN, J. 2006 An overview of projection methods for incompressible flows. *Comput. Meth. Appl. Mech. Engng* **195**, 6011–6045.

HALEY, P. J. & LERMUSIAUX, P. F. J. 2010 Multiscale two-way embedding schemes for free-surface primitive equations in the 'Multidisciplinary Simulation, Estimation and Assimilation System'. *Ocean Dyn.* **60**, 1497–1537.

HÄRTEL, C., MEIBURG, E. & NECKER, F. 2000 Analysis and direct numerical simulation of the flow at a gravity-current head. Part 1. Flow topology and front speed for slip and no-slip boundaries. *J. Fluid. Mech.* **418**, 189–212.

HOLMES, P., LUMLEY, J. & BERKOOZ, G. 1996 *Turbulence, Coherent Structures, Dynamical Systems and Symmetry*. Cambridge University Press.

JABERI, F. A., MILLER, R. S., MADNIA, C. K. & GIVI, P. 1996 Non-Gaussian scalar statistics in homogeneous turbulence. *J. Fluid Mech.* **313**, 241–282.

JANSEN, P. 2003 Nonlinear four-wave interactions and freak waves. *J. Phys. Oceanogr.* **33**, 863–884.

KNIO, O. M. & LE MAITRE, O. P. 2006 Uncertainty propagation in CFD using polynomial chaos decomposition. *Fluid Dyn. Res.* **38**, 616–640.

KUNDU, P. K., COHEN, I. M. & DOWLING, D. R. 2012 *Fluid Mechanics*, 5th edn. Academic Press.

LALL, S., MARSDEN, J. E. & GLAVASKI, S. 2002 A subspace approach to balanced truncation for model reduction of nonlinear control systems. *Intl J. Robust Nonlinear Control* **12**, 519–535.

LERMUSIAUX, P. F. J. 2006 Uncertainty estimation and prediction for interdisciplinary ocean dynamics. *J. Comput. Phys.* **217**, 176–199.

LERMUSIAUX, P. F. J., CHIU, C.-S, GAWARKIEWICZ, G. G., ABBOT, P., ROBINSON, A. R., MILLER, R. N., HALEY, P. J., LESLIE, W. G., MAJUMDAR, S. J., PANG, A. & LEKIEN, F. 2006 Quantifying uncertainties in ocean predictions. *Oceanography* **19**, 92–105.

LERMUSIAUX, P. F. J., CHIU, C.-S. & ROBINSON, A. R. 2002 Modelling uncertainties in the prediction of the acoustic wavefield in a shelfbreak environment. In *Proceedings of the 5th International Conference in Theoretical and Computational Acoustics, 21–25 May 2001* (ed. E.-C. Shang, Q. Li & T. F. Gao), pp. 191–200. World Scientific.

LI, Y. & MENEVEAU, C. 2005 Origin of non-Gaussian statistics in hydrodynamic turbulence. *Phys. Rev. Lett.* **95**, 164502.

MA, Z., ROWLEY, C. W. & TADMOR, G. 2010 Snapshot-based balanced truncation for linear time-periodic systems. *IEEE Trans. Autom. Control* **55**, 469–473.

LE MAITRE, O. P., KNIO, O. M., NAJM, H. & GHANEM, R. 2001 A stochastic projection method for fluid flow: basic formulation. *J. Comput. Phys.* **173**, 481–511.

MAJDA, A. J. & BRANICKI, M. 2012 Lessons in uncertainty quantification for turbulent dynamical systems. *Discrete Continuous Dyn. Syst.* **32**, 3133–3221.

MARSCH, E. & TU, C.-Y. 1997 Intermittency, non-Gaussian statistics and fractal scaling of MHD fluctuations in the solar wind. *Nonlinear Process. Geophys.* **4**, 101–124.

MONIN, A. & YAGLOM, A. 1971 *Statistical Fluid Mechanics: Mechanics of Turbulence*, I, II, MIT.

NOACK, B. R., AFANASIEV, K., MORZYNSKI, M., TADMOR, G. & THIELE, F. 2003 A hierarchy of low-dimensional models for the transient and post-transient cylinder wake. *J. Fluid. Mech.* **497**, 335–363.

PALLARES, J., GRAU, F. X. & GIRALT, F. 1999 Flow transitions in laminar Rayleigh–Bénard convection in a cubical cavity at moderate Rayleigh numbers. *Intl J. Heat Mass Transfer* **42**, 753–769.

REMPFER, D. & FASEL, H. F. 1994 Dynamics of three-dimensional coherent structures in a flat-plate boundary layer. *J. Fluid Mech.* **275**, 257–283.

ROACHE, P. J. 1997 Quantification of uncertainty in computational fluid dynamics. *Annu. Rev. Fluid Mech.* **29**, 123–160.

SAPSIS, T. P. 2013 Attractor local dimensionality, nonlinear energy transfers, and finite-time instabilities in unstable dynamical systems with applications to 2D fluid flows. *Proc. R. Soc. Lond.* A **469** (2153), 20120550.

SAPSIS, T. P. & LERMUSIAUX, P. F. J. 2009 Dynamically orthogonal field equations for continuous stochastic dynamical systems. *Physica* D **238**, 2347–2360.

SAPSIS, T. P. & LERMUSIAUX, P. F. J. 2012 Dynamical criteria for the evolution of the stochastic dimensionality in flows with uncertainty. *Physica* D **241**, 60–76.

SAPSIS, T. P. & MAJDA, A. J. 2013*a* Blended reduced subspace algorithms for uncertainty quantification of quadratic systems with a stable mean state. *Physica* D **258**, 61–76.

SAPSIS, T. P. & MAJDA, A. J. 2013*b* Blending modified Gaussian closure and non-Gaussian reduced subspace methods for turbulent dynamical systems. *J. Nonlinear Sci.* (in press). doi:10.1007/s00332-013-9178-1.

SAPSIS, T. P. & MAJDA, A. J. 2013*c* A statistically accurate modified quasilinear Gaussian closure for uncertainty quantification in turbulent dynamical systems. *Physica* D **252**, 34–45.

SCHERTZER, D. & LOVEJOY, S. 1987 Physically based rain and cloud modelling by anisotropic multiplicative turbulent cascades. *J. Geophys. Res.* **92**, 9693–9714.

SIROVICH, L. 1987 Turbulence and the dynamics of coherent structures. Parts I, II and III. *Q. Appl. Maths* **XLV**, 561–590.

SURA, P. 2010 On non-Gaussian SST variability in the Gulf Stream and other strong currents. *Ocean Dyn.* **60**, 155–170.

TADMOR, G., LEHMANN, O., NOACK, B. R., CORDIER, L., DELVILLE, J., BONNET, J. P. & MORZYNSKI, M. 2011 Reduced order models for closed-loop wake control. *Phil. Trans. R. Soc.* A **369**, 1513–1524.

TADMOR, G., LEHMANN, O., NOACK, B. R. & MORZYNSKI, M. 2010 Mean field representation of the natural and actuated cylinder wake flow. *Phys. Fluids* **22**, 034102.

UECKERMANN, M. P., LERMUSIAUX, P. F. J. & SAPSIS, T. P. 2013 Numerical schemes for dynamically orthogonal equations of stochastic fluid and ocean flows. *J. Comput. Phys.* **233**, 272–294.

VENTURI, D., WAN, X. & KARNIADAKIS, G. 2008 Stochastic low-dimensional modelling of a random laminar wake past a circular cylinder. *J. Fluid Mech.* **606**, 339–367.

VENTURI, D., WAN, X. & KARNIADAKIS, G. 2010 Stochastic bifurcation analysis of Rayleigh–Bénard convection. *J. Fluid Mech.* **650**, 391–413.

VINCENT, A. & MENEGUZZI, M. 1991 The spatial structure and statistical properties of homogeneous turbulence. *J. Fluid Mech.* **225**, 1–20.

XIU, D. & KARNIADAKIS, G. 2003 Modelling uncertainty in flow simulations via generalized polynomial chaos. *J. Comput. Phys.* **187**, 137–167.

ZORICH, V. A. 2004 *Mathematical Analysis*, II, Springer.